Chapter 12

Middle Atmosphere Dynamics

The *middle atmosphere* is generally regarded as the region extending from the tropopause (about 10–16 km altitude, depending on latitude) to about 100 km. The bulk of the middle atmosphere consists of two main layers, the *stratosphere* and the *mesosphere*, which are distinguished on the basis of temperature stratification (Figure 12.1). The stratosphere, which has large static stability associated with an overall increase of temperature with height, extends from the tropopause to the *stratopause* at about 50 km. The mesosphere, which has a lapse rate similar to that in the troposphere, extends from the stratopause to the *mesopause* at about 80 to 90 km.

Previous chapters of this text have focused almost exclusively on the dynamics of the troposphere. The troposphere accounts for about 85% of the total mass of the atmosphere and virtually all atmospheric water. There can be little doubt that processes occurring in the troposphere are primarily responsible for weather disturbances and climate variability. Nevertheless the middle atmosphere cannot be neglected. The troposphere and the middle atmosphere are linked through radiative and dynamical processes that must be represented in global forecast and climate models. They are also linked through the exchange of trace substances that are important in the photochemistry of the ozone layer. This chapter focuses primarily on dynamical processes in the lower part of the middle atmosphere and their links to the troposphere.

12.1 STRUCTURE AND CIRCULATION OF THE MIDDLE ATMOSPHERE

Zonal-mean temperature cross-sections for January and July in the lower and middle atmosphere are shown in the upper panels of Figures 12.2 and 12.3, respectively. Because very little solar radiation is absorbed in the troposphere, the thermal structure of the troposphere is maintained by an approximate balance among infrared radiative cooling, vertical transport of sensible and latent heat away from the surface by small-scale eddies, and large-scale heat transport by synoptic-scale eddies. The net result is a mean temperature structure in which the surface temperature has its maximum in the equatorial region and decreases

An Introduction to Dynamic Meteorology. DOI: 10.1016/B978-0-12-384866-6.00012-X
Copyright © 2013 Elsevier Inc. All rights reserved.

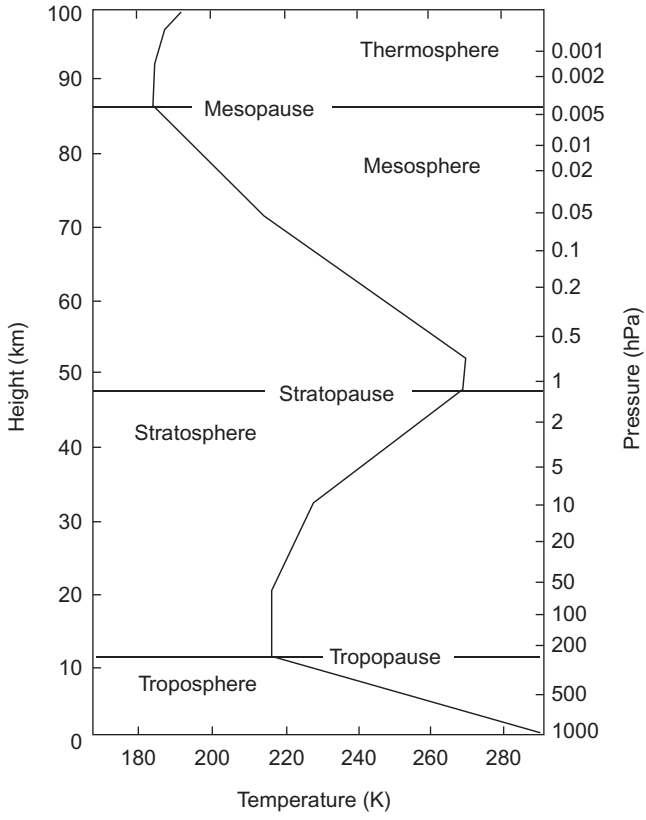

FIGURE 12.1 Midlatitude mean temperature profile. (*Based on the U.S. Standard Atmosphere, 1976.*)

toward both the winter and the summer poles. There is also a rapid decrease in altitude, with a lapse rate of about $6^{\circ}\mathrm{C\,km^{-1}}$.

In the stratosphere, however, infrared radiative cooling is in the mean balanced primarily by radiative heating due to the absorption of solar ultraviolet radiation by ozone. As a result of the solar heating in the ozone layer, the mean temperature in the stratosphere increases with height to a maximum at the stratopause near 50 km. Above the stratopause, temperature decreases with height due to the reduced solar heating of ozone.

The meridional temperature structure in the middle atmosphere is also quite different from that in the troposphere. In the lower stratosphere, where the temperature is strongly influenced by upper tropospheric processes, there is a temperature minimum at the equator and maxima at the summer pole and in midlatitudes of the winter hemisphere. Above about 30 hPa the temperature decreases uniformly from summer pole to winter pole, in qualitative accord with radiative equilibrium conditions.

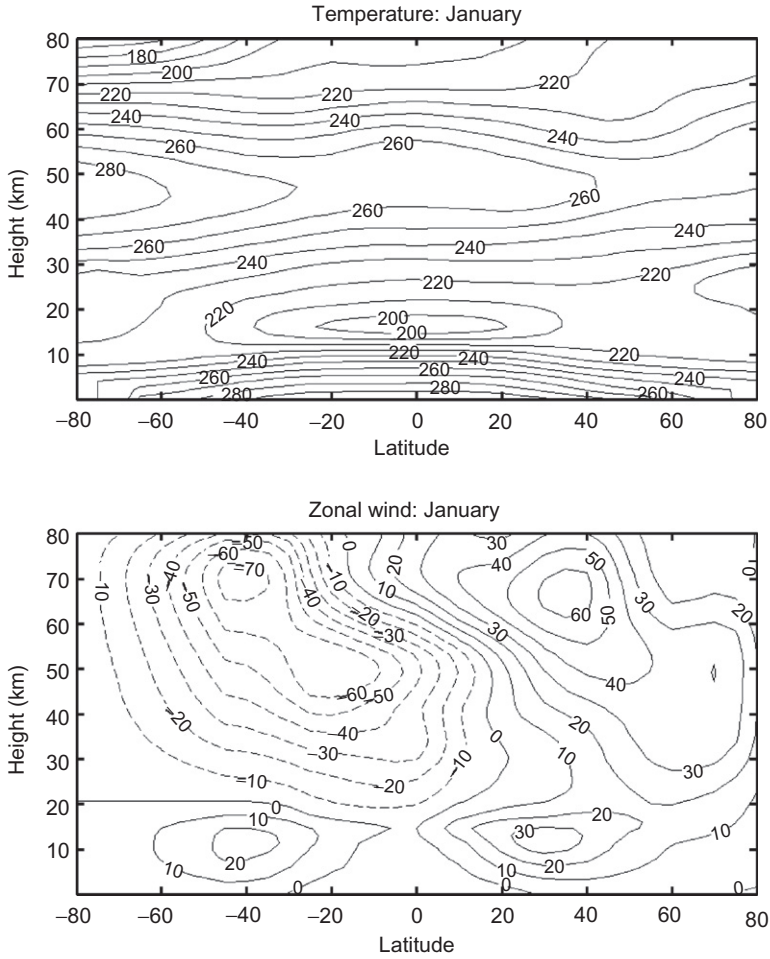

FIGURE 12.2 Observed monthly and zonally averaged temperature (K) and zonal wind ($m\,s^{-1}$) for January. (*Based on Fleming et al., 1990.*)

Mean zonal wind climatologies for the middle atmosphere are usually derived from the satellite-observed temperature field. This is done using the geostrophic winds on an isobaric surface in the lower stratosphere (obtained from conventional meteorological analyses) as a lower boundary condition and integrating the thermal wind equation vertically. January and July mean zonal wind cross-sections are shown in the lower panels of Figures 12.2 and 12.3, respectively. The main features are an easterly jet in the summer hemisphere and a westerly jet in the winter hemisphere, with maxima in the wind speeds occurring near the 60-km level. Of particular significance are the high-latitude westerly jets in the winter hemispheres. These polar night jets provide wave

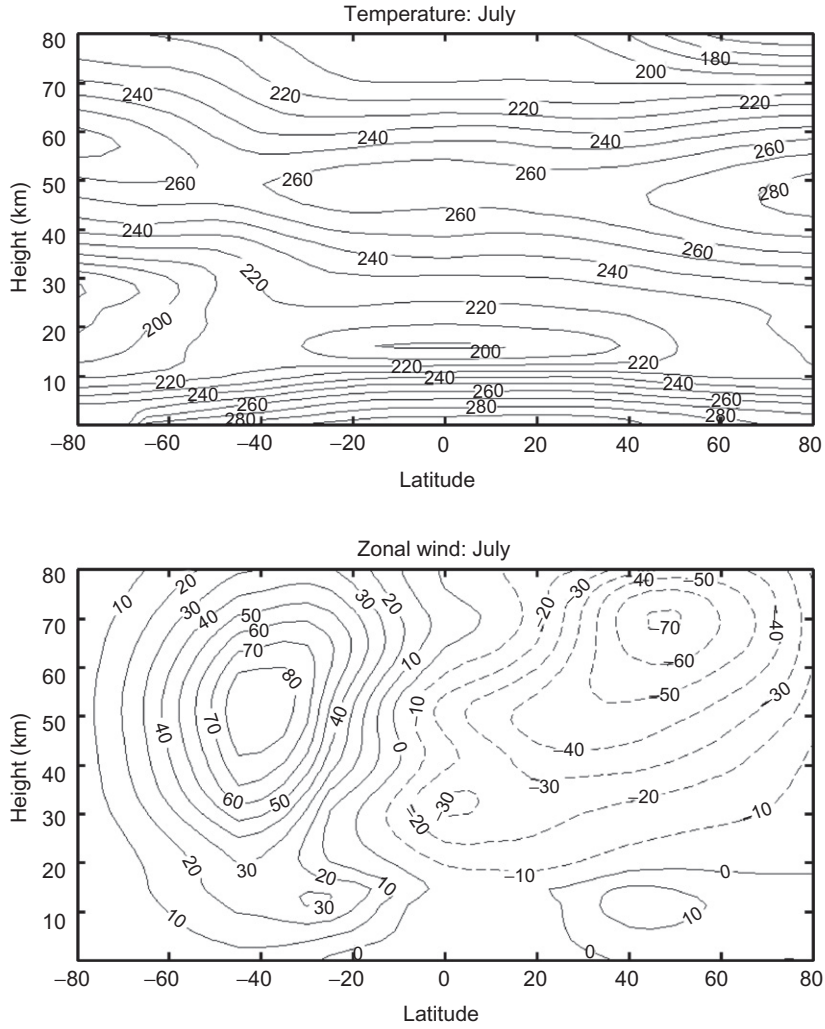

FIGURE 12.3 Observed monthly and zonally averaged temperature (K) and zonal wind ($m\,s^{-1}$) for July. (*Based on Fleming et al., 1990.*)

guides for the vertical propagation of quasi-stationary planetary waves. In the Northern Hemisphere the EP flux convergence (see Section 10.2.2) due to such waves occasionally leads to rapid deceleration of the mean zonal flow and an accompanying *sudden stratospheric warming* in the polar region, as discussed in Section 12.4.

The zonal mean flow in the equatorial middle atmosphere is strongly influenced by vertically propagating inertia–gravity waves and by equatorial wave

modes, especially the Kelvin and Rossby–gravity modes. These waves interact with the mean flow to produce a long-period oscillation called *quasi-biennial oscillation*. This oscillation produces large year-to-year variability in the mean zonal wind in the equatorial middle atmosphere, which is not shown in the long-term means of Figure 12.3.

12.2 THE ZONAL-MEAN CIRCULATION OF THE MIDDLE ATMOSPHERE

As discussed in Section 10.1, the general circulation of the atmosphere considered as a whole can be regarded to a first approximation as the atmospheric response to the diabatic heating caused by absorption of solar radiation at the surface. Thus, it is reasonable to say that the atmosphere is driven by differential diabatic heating. For an open subregion of the atmosphere, such as the middle atmosphere, it is not correct, however, to assume that the circulation is driven by diabatic heating. It is, rather, necessary to consider the transfer of momentum and energy between that subregion and the rest of the atmosphere.

In the absence of eddy motions, the zonal-mean temperature of the middle atmosphere would relax to a radiatively determined state in which, except for a small lag due to thermal inertia, the temperature would correspond to an annually varying radiative equilibrium following the annual cycle in solar heating. The circulation in such a situation would consist only of a zonal-mean zonal flow in thermal wind balance with the meridional temperature gradient. Neglecting small effects of the annual cycle, there would be no meridional or vertical circulation and no stratosphere–troposphere exchange for such a hypothetical state.

A cross-section of the radiatively determined temperature during a Northern Hemisphere winter is shown in Figure 12.4. It should be compared to the observed temperature profile for the same season that was shown in Figure 12.2. Although the rather uniform increase of temperature from winter pole to summer pole in the region of 30- to 60-km altitude is qualitatively consistent with the radiatively determined distribution, the actual temperature difference between the two poles is much smaller than in the radiatively determined state. Above 60 km even the sign of the gradient is opposite to that in the radiative solution; the observed temperatures near the summer polar mesopause are much colder than those near the winter polar mesopause.

Departures from this radiatively determined state must be maintained by eddy transports. Thus, rather than *causing* the mean circulation, the radiative heating and cooling patterns observed in the middle atmosphere are a *result* of the eddies driving the flow away from a state of radiative balance. This eddy-driven circulation has meridional and vertical wind components that induce substantial local departures from radiative equilibrium, especially in the winter stratosphere and in the mesosphere in both winter and summer.

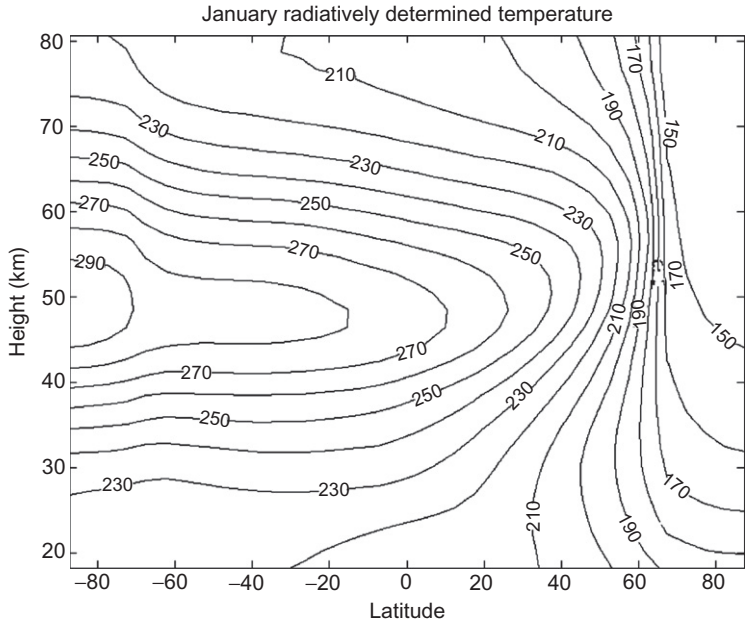

FIGURE 12.4 Radiatively determined middle atmosphere temperature distribution (K) for northern winter soltice from a radiative model that is time-marched through an annual cycle. Realistic tropospheric temperatures and cloudiness are used to determine the upward radiative flux at the tropopause. (*Based on Shine, 1987.*)

12.2.1 Lagrangian Motion of Air Parcels

Viewed in the conventional Eulerian mean framework (Section 10.2.1), the time-averaged zonal-mean temperature distribution in the middle atmosphere is determined by the net balance among net radiative heating or cooling, eddy heat transport, and adiabatic heating or cooling by the mean meridional circulation ($\overline{v}, \overline{w}$). That this framework does not provide a useful model for transport in the meridional plane can be seen easily by considering steady-state adiabatic motion in the presence of large-scale waves. According to (10.12), in such a situation waves that have a positive poleward heat flux must drive a nonzero $\overline{w}$, with upwelling at high latitudes and downwelling at low latitudes corresponding to the regions of heat flux convergence and divergence, respectively. However, if the flow is adiabatic, there can be no motion across the isentropes, and thus in steady state there can be no net vertical transport even though $\overline{w}$ is nonzero. Thus, $\overline{w}$ clearly does not provide an approximation to the vertical motion of air parcels (i.e., the vertical transport) in such a situation.

But how can vertical transport vanish when the Eulerian mean vertical motion is finite? The resolution of this "nontransport" paradox can be illustrated by considering the kinematics of adiabatic flow in the presence of a stationary

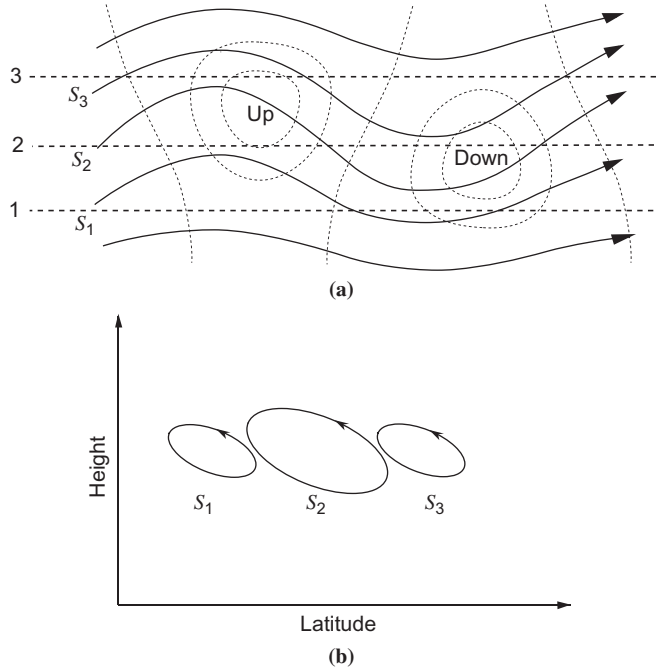

FIGURE 12.5 Parcel motions for an adiabatic planetary wave in a westerly zonal flow. (a) *Solid lines* labeled S_1, S_2, and S_3 are parcel trajectories, *heavy dashed lines* are latitude circles, and *light dashed lines* are contours of the vertical velocity field. (b) Projection of parcel oscillations on the meridional plane.

large-scale wave superposed on a background westerly flow as shown in Figure 12.5a. Parcels moving along the streamlines labeled S_1, S_2, and S_3 will oscillate about their mean latitudes, moving equatorward and upward, then poleward and downward following the up and down displacements of the isentropic surfaces associated with the wave. However, over a full wave period there can be no net vertical motion following the parcels, as the parcels must remain on the same isentropic surface. Hence there can be no vertical transport. If, however, an average vertical velocity is computed by taking the mean along a constant latitude circle, then as clearly shown in Figure 12.5a, on the latitude circle ϕ_3 poleward of the maximum in wave amplitude, the Eulerian mean is upward, $\overline{w}(\phi_3) > 0$, as regions of upward motion dominate over regions of downward motion at that latitude.

Conversely, on the latitude circle ϕ_1 equatorward of the maximum in wave amplitude, the Eulerian mean is downward $\overline{w}(\phi_1) < 0$. The conventional Eulerian mean circulation thus suggests misleadingly that a trace constituent would be transported upward poleward of the latitude of maximum wave amplitude and downward equatorward of that latitude. In reality, air parcels in this idealized example of adiabatic wave motion are not undergoing net vertical

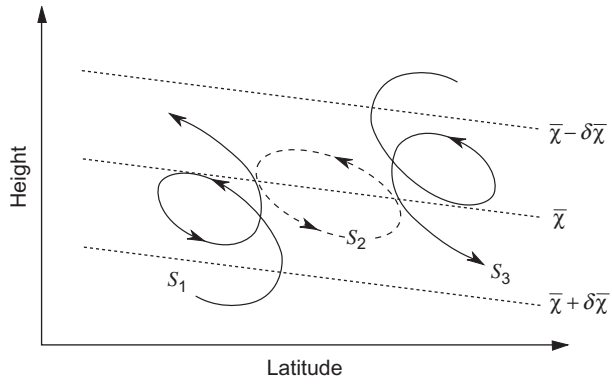

FIGURE 12.6 Projections of parcel motions on the meridional plane for planetary waves in westerlies with diabatic heating at low latitudes and diabatic cooling at high latitudes. *Thin dashed lines* show tilting of isosurfaces of tracer mixing ratio due to transport by the diabatic circulation.

displacements, but are simply oscillating back and forth along the same isentropic surface with trajectories whose meridional projections are closed ellipses as shown in Figure 12.5b. In such a situation there is no net vertical parcel motion, and thus no net vertical transport.

Only if there is net diabatic heating or cooling can there be mean transport across the isentropes. In the winter stratosphere, where stationary planetary wave amplitudes tend to be large and there is diabatic heating at low latitudes and diabatic cooling at high latitudes, the meridional projection of actual parcel motions is a combination of the elliptical orbits of Figure 12.5b and mean vertical drift as indicated in Figure 12.6, which clearly shows that a vertically stratified long-lived trace constituent is transported upward at low latitudes and downward at high latitudes because of vertical transport of fluid parcels associated with diabatic heating and cooling. Thus, in order to represent net transport effects efficiently, a zonal averaging process should yield an average vertical circulation that mimics the net cross-isentropic parcel motion.

12.2.2 The Transformed Eulerian Mean

In many circumstances the transformed Eulerian mean (TEM) equations introduced in Section 10.2.2 provide a useful model for the study of global-scale middle atmospheric transport. Recall that in this formulation the zonal-mean momentum, mass continuity, thermodynamic energy, and thermal wind equations have the form[1]

$$\partial\overline{u}/\partial t - f_0\overline{v}^* = \rho_0^{-1}\,\nabla\cdot\mathbf{F} + \overline{X} \equiv \overline{G} \tag{12.1}$$

[1] As in Chapter 10, we express the log-pressure coordinate simply as z rather than z^*.

$$\partial \overline{T}/\partial t + N^2 H R^{-1} \overline{w}^* = -\alpha_r \left[\overline{T} - \overline{T}_r\,(y, z, t)\right] \tag{12.2}$$

$$\partial \overline{v}^*/\partial y + \rho_0^{-1} \partial\left(\rho_0 \overline{w}^*\right)/\partial z = 0 \tag{12.3}$$

$$f_0 \partial \overline{u}/\partial z + R H^{-1} \partial \overline{T}/\partial y = 0 \tag{12.4}$$

Here the residual circulation $(\overline{v}^*, \overline{w}^*)$ is as defined in (10.16a,b), $\mathbf{F}$ designates the EP flux due to large-scale eddies, $\overline{X}$ is the zonal force due to small-scale eddies (e.g., gravity wave drag), and $\overline{G}$ designates the total *zonal force*. In (12.2) the diabatic heating is approximated in terms of a Newtonian relaxation proportional to the departure of the zonal mean temperature $\overline{T}(y, z, t)$ from its radiative equilibrium value $\overline{T_r}(y, z, t)$, where α_r is the Newtonian cooling rate.

To understand how eddies can lead to departures of the zonal-mean temperature distribution in the middle atmosphere from its radiatively determined state, we use the TEM system of equations to consider an idealized model of extratropical forcing. The dependence of the circulation on forcing frequency can be examined in an idealized model in which $\overline{T}_r$ is taken to be a function of height alone, and the forcing has a simple harmonic dependence in time with frequency σ. Then $\overline{w}^*$ and $\overline{G}$ are of the form

$$\begin{bmatrix} \overline{w}^* \\ \overline{G} \end{bmatrix} = Re \begin{bmatrix} \hat{w}\,(\phi, z) \\ \hat{G}\,(\phi, z) \end{bmatrix} e^{i\sigma t} \tag{12.5}$$

where $\hat{w}$ and $\hat{G}$ are complex latitude- and height-dependent amplitudes. Combining (12.1) and (12.3) to eliminate $\overline{v}^*$ and combining the resulting equation with (12.2) and (12.4) to eliminate $\overline{T}$ yields a partial differential equation for $\hat{w}$:

$$\frac{\partial}{\partial z}\left(\frac{1}{\rho_0}\frac{\partial\left(\rho_0 \hat{w}\right)}{\partial z}\right) + \left(\frac{i\sigma}{i\sigma + \alpha_r}\right)\left(\frac{N^2}{f_0^2}\right)\frac{\partial^2 \hat{w}}{\partial y^2} = \frac{1}{f_0}\frac{\partial}{\partial y}\left(\frac{\partial \hat{G}}{\partial z}\right) \tag{12.6}$$

The structure of $\hat{w}$ in the meridional plane depends on the latitudinal and vertical distribution of the forcing $\hat{G}$. The differential equation (12.6) is elliptic in form. Such a form implies that a forcing applied locally in any region will produce a nonlocal response in the form of a large-scale circulation that acts to maintain the zonal flow in thermal wind balance with the meridional temperature gradient.

As suggested by the coefficients of (12.6), the character of the nonlocal response depends on the ratio of the frequency of the forcing to the Newtonian relaxation rate. We consider three cases:

1. *High-frequency variations* $\sigma \gg \alpha_r$: The motions are approximately adiabatic (as is true in sudden stratospheric warmings)—that is,

$$\frac{i\sigma}{i\sigma + \alpha_r} \to 1$$

Away from the forcing region, the right side of (12.6) vanishes so that the two terms on the left must balance each other. For this balance to hold, a simple scaling argument indicates that in midlatitudes the vertical scale δz of the response must be related to the horizontal scale as $\delta z \sim (f_0/N)\,\delta y \sim 10^{-2}\delta y$.

2. *Low-frequency variations (e.g., the annual cycle)*: The Newtonian relaxation coefficient has a magnitude of order $\alpha_r \approx 1/(20 \text{ days})$ in the lower stratosphere, increasing to $\alpha_r \approx 1/(5 \text{ days})$ near the stratopause. Thus $\alpha_r > \sigma$ and the coefficient multiplying the second term on the left in (12.6) is reduced from its value in case (1) so that the vertical penetration scale is increased.
3. *Steady-state regime* $\sigma/\alpha_r \to 0$: In this limit $\partial\overline{u}/\partial t = 0$, and rather than using (12.6), it is simpler to note that (12.1) in this case reduces to a simple balance between the Coriolis force and the zonal drag force:

$$-f_0\overline{v}^* = \overline{G} \tag{12.7}$$

Combining this equation with the continuity equation (12.3) and requiring that

$$\rho_0\overline{w}^* \to 0 \quad \text{as} \quad z \to \infty$$

it follows that

$$\rho_o\overline{w}^* = -\frac{\partial}{\partial y}\left[\frac{1}{f_0}\int_z^\infty \rho_0\overline{G}dz'\right] \tag{12.8}$$

According to (12.8), $\overline{w}^*$ is zero in the regions *above* a localized forcing region, whereas it is constant for regions directly below it; hence the term *downward control* is sometimes used to refer to this steady-state situation.

Substitution of (12.8) into the first law of thermodynamics (12.2) and neglecting the time-dependent term yield an expression that explicitly shows the dependence on the zonal force distribution of the departure of the time and zonally averaged temperature from radiative equilibrium:

$$\left(\overline{T} - \overline{T}_r\right) = \frac{N^2H}{\alpha_r\rho_0R}\frac{\partial}{\partial y}\left[\frac{1}{f_0}\int_z^\infty \rho_0\overline{G}dz'\right] \tag{12.9}$$

Thus, in steady state the departure of temperature from radiative equilibrium at a given level depends on the meridional gradient of the zonal force distribution in the column above that level.

For mathematical simplicity, the variation of the Coriolis parameter with latitude and other effects of spherical geometry have been neglected in deriving the equations of this section. It is straightforward to extend this model to spherical coordinates. Figure 12.7 shows streamlines of the meridional mass circulation

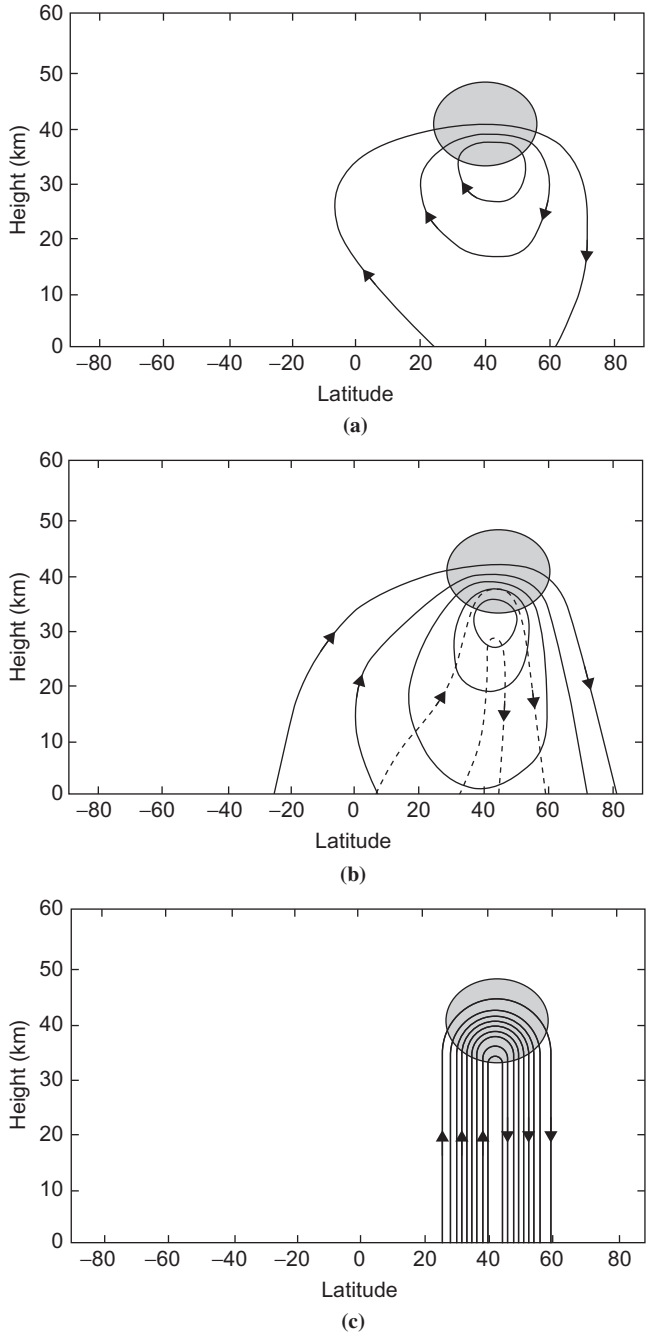

FIGURE 12.7 Response of the zonally symmetric circulation to a westward force applied in the *shaded* region. Contours are *streamlines* of the TEM meridional circulation, with the same contour interval used in each panel. (a) Adiabatic response for high-frequency forcing. (b) Response for annual frequency forcing and 20-day radiative damping timescale; *solid and dashed contours* show the response that is in phase and 90° out of phase, respectively, with the forcing. (c) Response to steady-state forcing. (*After Holton et al., 1995. Used with permission of American Geophysical Union.*)

in response to isolated extratropical forcing for three cases corresponding to the differing frequency regimes discussed earlier, but with spherical geometry retained.

A comparison of Figures 12.2 and 12.4 shows that the largest departures from radiative equilibrium occur in the summer and winter mesosphere and in the polar winter stratosphere. According to (12.9), these are the locations and seasons when zonal forcing must be strongest. The zonal force in the mesosphere is believed to be caused primarily by vertically propagating internal gravity waves. These transfer momentum from the troposphere into the mesosphere, where wave breaking produces strong zonal forcing. The zonal force in the winter stratosphere is due primarily to stationary planetary Rossby waves. These, as discussed in Section 12.3, can propagate vertically provided that the mean zonal wind is westerly and less than a critical value that depends strongly on the wavelength of the waves. Thus, in the extratropical stratosphere we expect a strong annual cycle in $\delta\overline{T}$, with large values (i.e., strong departure from radiative equilibrium) in winter and small values in summer.

This is indeed observed (see Figures 12.2 and 12.4). Furthermore, because eddy forcing maintains the observed temperature above its radiative equilibrium in the extratropical stratosphere, there is radiative cooling, and from (12.3) the residual vertical motion must be downward. By mass continuity it is then required that the residual vertical motion be upward in the tropics, implying that the temperature must be below radiative equilibrium in that region. Note that it is the dynamical driving by extratropical eddies, rather than local forcing, that is responsible for the upward residual motion and net radiative heating in the tropical stratosphere.

12.2.3 Zonal-Mean Transport

Viewed from the TEM perspective, the overall meridional circulation in the winter stratosphere is qualitatively as pictured in Figure 12.8. The residual circulation transfers mass and trace chemicals upward across the tropopause in the tropics and downward in the extratropics. This vertical circulation is closed in the lower stratosphere by a poleward meridional drift balanced by EP flux convergence. That this schematic picture gives a qualitatively correct view can be ascertained by examining the zonal-mean mixing ratio distribution of any long-lived vertically stratified trace species. As an example, the distribution of N_2O is shown in Figure 12.9. N_2O is produced at the surface and is mixed uniformly in the troposphere, but then it decays with height in the stratosphere due to photochemical dissociation. Thus, as shown in Figure 12.9, the mixing ratio decreases upward in the stratosphere. Note, however, that surfaces of constant mixing ratio are displaced upward in the tropics and downward at higher latitudes, suggesting that the mean meridional mass transport is upward in the tropics and downward in the extratropics as suggested in Figure 12.9.

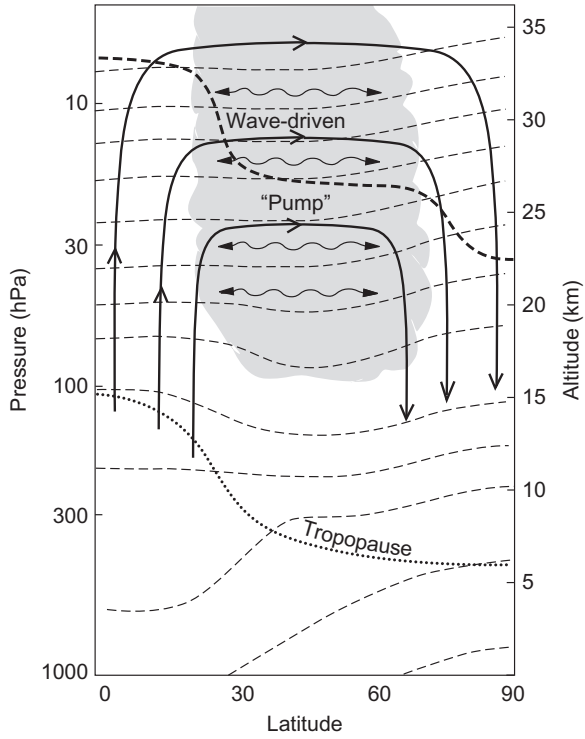

FIGURE 12.8 Schematic cross-section of the wave-driven circulation in the middle atmosphere and its role in transport. *Thin dashed lines* denote potential temperature surfaces. *Dotted line* is the tropopause. *Solid lines* are contours of the TEM meridional circulation driven by the wave-induced forcing (*shaded region*). *Wavy double-headed arrows* denote meridional transport and mixing by eddy motions. *Heavy dashed line* shows an isopleth of mixing ratio for a long-lived tracer.

In addition to the slow meridional drift by the residual meridional velocity shown in Figure 12.8, tracers in the winter stratosphere are also subject to rapid quasi-isentropic transport and mixing by breaking planetary waves. Such eddy transport, which is highly variable in space and time, must be included for quantitatively accurate modeling of transport within the stratosphere.

In the mesosphere the residual circulation is dominated by a single circulation cell with upward motion in the summer polar region, meridional drift from the summer to the winter hemisphere, and subsidence in the winter polar region. This circulation, like the residual circulation in the stratosphere, is eddy driven. However, in the mesosphere it appears that the dominant eddies are vertically propagating internal gravity waves, which have shorter scales in space and time than the planetary waves that dominate the eddy activity in the stratosphere.

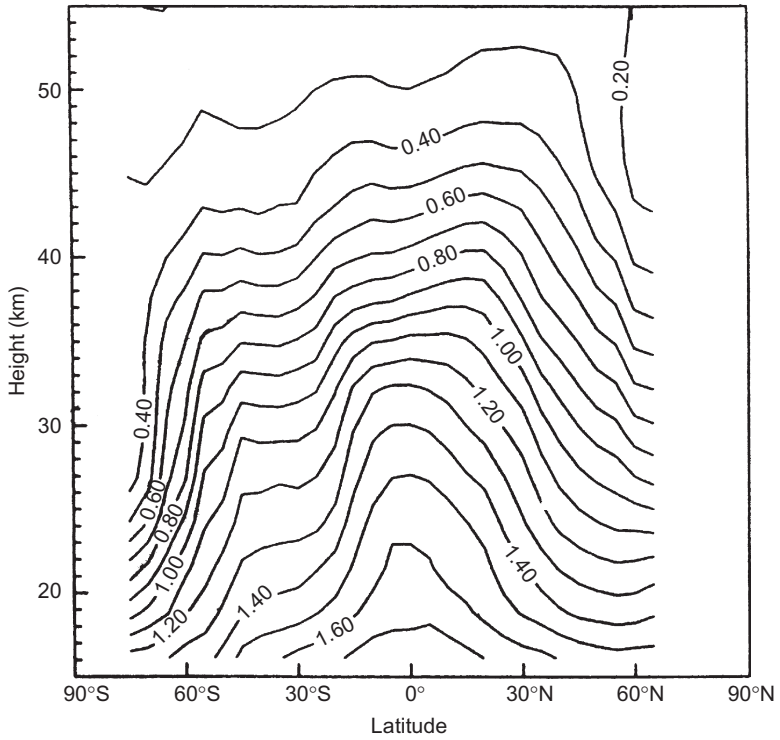

FIGURE 12.9 October zonal mean cross-section of methane (ppmv) from observations by the HALOE on the UARS. Note the strong vertical stratification due to photochemical destruction in the stratosphere. The upward-bulging mixing ratio isopleths in the equatorial region are evidence of upward mass flow in the equatorial region, whereas the downward-sloping isopleths in high latitudes are evidence of subsidence in the polar regions. The region of flattened isopleths in the midlatitudes of the Southern Hemisphere is evidence for quasi-adiabatic wave transport due to wintertime planetary wave activity. (*After Norton, 2003.*)

12.3 VERTICALLY PROPAGATING PLANETARY WAVES

In Section 12.1 we pointed out that the predominant eddy motions in the stratosphere are vertically propagating quasi-stationary planetary waves (Rossby waves) and that these waves are confined to the winter hemisphere. To understand the absence of synoptic-scale motions and the confinement of stationary planetary waves to the winter hemisphere, it is necessary to examine the conditions under which planetary waves can propagate vertically.

12.3.1 Linear Rossby Waves

To analyze planetary wave propagation in the stratosphere, it is convenient to write the equations of motion in the log-pressure coordinate system introduced

in Section 7.4.1. For analysis of extratropical planetary wave motions in the middle atmosphere, we may refer the motions to the midlatitude β plane and use the quasi-geostrophic potential vorticity equation, which in log-pressure coordinates can be written as

$$\left(\frac{\partial}{\partial t} + \mathbf{V}_g \cdot \nabla\right) q = 0 \tag{12.10}$$

where

$$q \equiv \nabla^2 \psi + f + \frac{f_0^2}{\rho_0 N^2} \frac{\partial}{\partial z}\left(\rho_0 \frac{\partial \psi}{\partial z}\right)$$

Here $\psi = \Phi / f_0$ is the geostrophic streamfunction and f_0 is a constant midlatitude reference value of the Coriolis parameter. We now assume that the motion consists of a small-amplitude disturbance superposed on a constant zonal-mean flow. Thus, letting $\psi = -\overline{u}y + \psi'$, $q = \overline{q} + q'$ and linearizing (12.10), we find that the perturbation q' field must satisfy

$$\left(\frac{\partial}{\partial t} + \overline{u}\frac{\partial}{\partial x}\right) q' + \beta \frac{\partial \psi'}{\partial x} = 0 \tag{12.11}$$

where

$$q' \equiv \nabla^2 \psi' + \frac{f_0^2}{\rho_0 N^2} \frac{\partial}{\partial z}\left(\rho_0 \frac{\partial \psi'}{\partial z}\right) \tag{12.12}$$

Equation (12.11) has solutions in the form of harmonic waves with zonal and meridional wave numbers k and l and zonal phase speed c_x:

$$\psi'(x, y, z, t) = \Psi(z)\, e^{i(kx+ly-kc_x t)+z/2H} \tag{12.13}$$

Here the factor $e^{z/2H}$ (which is proportional to $\rho_0^{-1/2}$) is included to simplify the equation for the vertical dependence. Substituting (12.13) into (12.11) yields

$$d^2\Psi/dz^2 + m^2\Psi = 0 \tag{12.14}$$

where

$$m^2 \equiv \frac{N^2}{f_0^2}\left[\frac{\beta}{(\overline{u} - \mathrm{c_x})} - \left(k^2 + l^2\right)\right] - \frac{1}{4H^2} \tag{12.15}$$

Referring back to Section 7.4, we recall that $m^2 > 0$ is required for vertical propagation, and in that case, m is the vertical wave number; that is, solutions of (12.14) have the form $\Psi(z) = Ae^{imz}$, where A is a constant amplitude and

the sign of m is determined by requiring that the vertical component of group velocity be positive. For stationary waves ($c_x = 0$), we see from (12.15) that vertically propagating modes can exist only for mean zonal flows that satisfy the condition

$$0 < \overline{u} < \beta \left[\left(k^2 + l^2 \right) + f_0^2 / \left(4N^2 H^2 \right) \right]^{-1} \equiv U_c \tag{12.16}$$

where U_c is called the *Rossby critical velocity*. Thus, vertical propagation of stationary waves can occur only in the presence of westerly winds weaker than a critical value that depends on the horizontal scale of the waves. In the summer hemisphere the stratospheric mean zonal winds are easterly so that stationary planetary waves are all trapped vertically.

In the real atmosphere the mean zonal wind is not constant, but depends on latitude and height. However, both observational and theoretical studies suggest that (12.16) still provides a qualitative guide for estimating vertical propagation of planetary waves, even though the actual critical velocity may be larger than indicated by the β-plane theory.

12.3.2 Rossby Wavebreaking

The term *wavebreaking* for Rossby waves simply refers to a rapid, irreversible deformation of material contours. Since by (12.10) potential vorticity is approximately conserved in Rossby waves, isolines of potential vorticity on isentropic surfaces approximate material contours, and wavebreaking can best be illustrated by considering the field of potential vorticity. Wavebreaking may occur when the disturbance fields reach amplitudes for which nonlinear effects can no longer be neglected in the dynamical equations. For example, if the flow is divided into mean and disturbance parts, and nonlinear terms are included, the equation for conservation of quasi-geostrophic potential vorticity (12.10) becomes

$$\left(\frac{\partial}{\partial t} + \overline{u} \frac{\partial}{\partial x} \right) q' + v' \frac{\partial \overline{q}}{\partial y} = -u' \frac{\partial q'}{\partial x} - v' \frac{\partial q'}{\partial y} \tag{12.17}$$

For steady waves propagating relative to the ground at zonal-phase speed c_x, the variation of phase in time and space is given by $\phi = k\,(x - c_x t)$, where k is the zonal wave number, and it is readily verified that

$$\frac{\partial}{\partial t} = -c_x \frac{\partial}{\partial x}$$

so that in the linearized version of (12.17) there is a balance between advection of the disturbance potential vorticity q' by the Doppler-shifted mean wind and

the advection of mean potential vorticity by the disturbance meridional wind:

$$(\overline{u} - c_x)\,\frac{\partial q'}{\partial x} = -v'\frac{\partial \overline{q}}{\partial y} \tag{12.18}$$

The validity of the linear approximation can thus be assessed by comparing the sizes of the two terms on the right side of (12.17) with either term in (12.18). Linearity holds provided that

$$\left|\overline{u} - c_x\right| \gg \left|u'\right| \tag{12.19a}$$

and

$$\partial \overline{q}/\partial y \gg \left|\partial q'/\partial y\right| \tag{12.19b}$$

Basically these criteria require that the slope of the material contours in the x, y plane must be small.

As indicated in (12.13), in an atmosphere with constant mean zonal wind, vertically propagating linear Rossby waves have amplitudes increasing exponentially in height. Thus, at some altitude the disturbance amplitude will become sufficiently large so that wavebreaking must occur. In the real atmosphere, however, the mean-zonal flow varies in both latitude and height, and this variation is crucial for understanding the distribution and mean-flow forcing provided by Rossby wavebreaking. The simplest example of Rossby wavebreaking occurs in the presence of a *critical surface* along which the Doppler-shifted phase speed of the wave vanishes ($\overline{u} - c_x = 0$). In that case (12.19a) cannot be satisfied even for small-amplitude waves.

For understanding wave behavior near critical lines it is helpful to generalize the Rossby wave analysis of Section 12.3.1 to a situation such as that shown in the seasonal mean cross-sections of Figure 12.2 in which the zonal wind depends on latitude and height, $\overline{u} = \overline{u}\,(y, z)$. The x and t dependence in (12.11) can then be separated by seeking solutions of the form

$$\psi' = e^{z/2H}\mathrm{Re}\left[\Psi\,(y, z)\,e^{ik(x-c_x t)}\right] \tag{12.20}$$

We obtain

$$\frac{\partial^2 \Psi}{\partial y^2} + \frac{f_0^2}{N^2}\frac{\partial^2 \Psi}{\partial z^2} + n_k^2 \Psi = 0 \tag{12.21}$$

where the small vertical variation of N^2 is neglected, and

$$n_k^2\,(y, z) = (\overline{u} - c_x)^{-1}\,\partial \overline{q}/\partial y - k^2 - f_0^2/\left(4H^2N^2\right) \tag{12.22}$$

Equation (12.21) has a form similar to that of the equation governing the two-dimensional propagation of light waves in a medium with variable refractive index, n_k. The propagation of linear Rossby wave EP flux in that case can be shown to be along rays that behave somewhat like light rays. Thus, wave activity will tend to propagate along rays that bend toward regions of large positive n_k^2 and avoid regions of negative n_k^2. For stationary Rossby waves ($c_x = 0$) of low zonal wave number, n_k^2 is positive in a region with westerly winds that are not too strong, and increases to infinity along a critical surface where the mean flow vanishes. Thus, the index of refraction for wave activity is positive in the winter hemisphere, but increases rapidly toward the equatorial zero wind line. As a result, Rossby wave activity tends to propagate upward and equatorward, and wavebreaking occurs in the vicinity of the equatorial critical line.

12.4 SUDDEN STRATOSPHERIC WARMINGS

In the lower stratosphere the temperature is a minimum at the equator and has maxima at the summer pole and at about 45° latitude in the winter hemisphere (see Figure 12.2). From thermal wind considerations the rapid decrease of temperature poleward of 45° in winter requires a zonal vortex with strong westerly shear with height.

In the Northern Hemisphere, every other year or so, this normal winter pattern of a cold polar stratosphere with a westerly vortex is interrupted in a spectacular manner in midwinter. Within the space of a few days the polar vortex becomes highly distorted and breaks down (see Figure 12.10) with an accompanying large-scale warming of the polar stratosphere, which can quickly reverse the meridional temperature gradient and (through thermal wind balance) create a circumpolar easterly current. Warmings of 40 K in a few days have occurred at the 50-hPa level.

Numerous observational studies of sudden warmings confirm that enhanced propagation of planetary waves from the troposphere, primarily zonal wave numbers 1 and 2, is essential for the development of the warmings. Since major warmings are observed primarily in the Northern Hemisphere, it is logical to conclude that enhanced wave propagation into the stratosphere is due to topographically forced waves, which are much stronger in the Northern Hemisphere than in the Southern Hemisphere. Even in the Northern Hemisphere, however, it is apparently only in certain winters that conditions are right to produce sudden warmings.

It is generally accepted that sudden warmings are an example of transient mean-flow forcing due to planetary wave driving. Section 10.2.3 showed that in order for planetary waves to decelerate the zonal-mean circulation, there must be a nonzero equatorward eddy potential vorticity flux (i.e., a net EP flux convergence). We further showed that for steady nondissipative waves, the divergence of the EP flux vanishes. For normal stationary planetary waves in the stratospheric polar night jet, this constraint should be at least approximately satisfied,

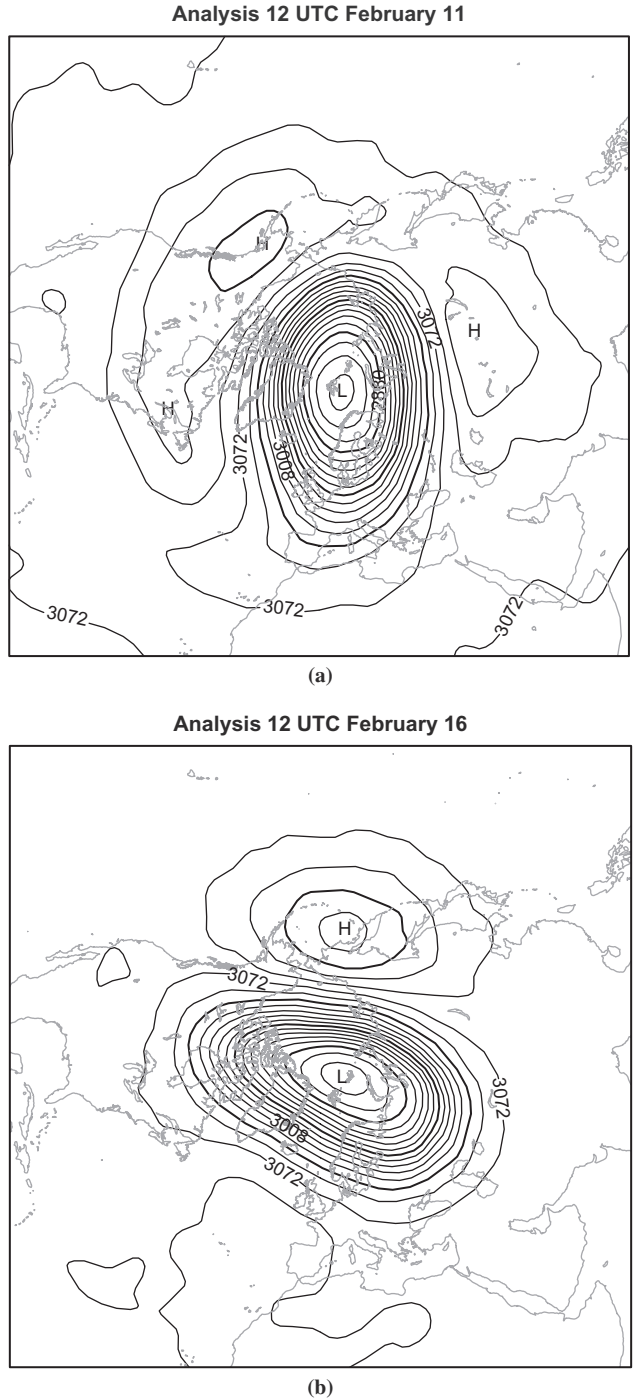

FIGURE 12.10 10-hPa geopotential height analyses for days in 1979: February 11 (a), February 16 (b), and February 21 (c) at 12 UTC, showing breakdown of the polar vortex associated with a wave number 2's sudden stratospheric warming. Contour interval: 16 dam. (*Analysis from ERA-40 reanalysis courtesy of the European Centre for Medium-Range Weather Forecasts.*)

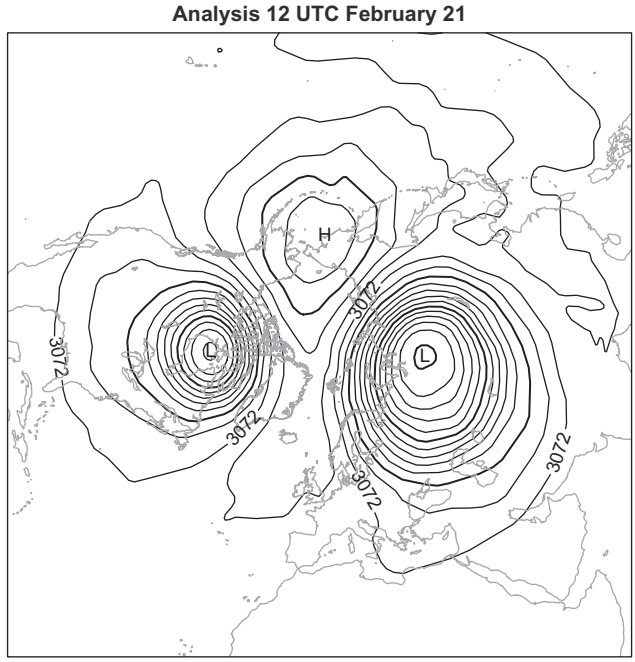

(c)

FIGURE 12.10 (continued)

as radiative and frictional dissipation are rather small. Thus, the strong interaction between the waves and the mean flow that occurs during the course of a sudden warming must be associated with wave transience (i.e., change of amplitude with respect to time) and wave dissipation. Most of the dramatic mean-flow deceleration that occurs during a sudden warming is caused by amplification of quasi-stationary planetary waves in the troposphere followed by propagation into the stratosphere.

This process can be understood by considering the interaction between zonal mean and eddy potential vorticities. We assume that on the short time scales characteristic of sudden warmings, diabatic processes can be neglected. We also assume that the eddy motion is approximately governed by the linearized eddy potential vorticity equation and that the zonal mean is changed only by the eddy flux convergence. The eddies and mean flow are thus related by the quasi-linear system

$$\left(\frac{\partial}{\partial t} + \overline{u}\,\frac{\partial}{\partial x}\right) q' + v'\frac{\partial \overline{q}}{\partial y} = -S' \tag{12.23}$$

where again

$$q' \equiv \nabla^2 \psi' + \frac{f_0^2}{\rho_0} \frac{\partial}{\partial z} \left(\frac{\rho_0}{N^2} \frac{\partial \psi'}{\partial z} \right) \tag{12.24}$$

and an eddy damping term, $-S'$, has been added to represent the effects of both mechanical and thermal dissipation. (For constant and equal Rayleigh friction and Newtonian cooling, $S' = \alpha q'$, where α is the dissipation rate coefficient.) Multiplying (12.23) by q' and averaging zonally after noting that

$$\overline{\bar{u}\, q' \frac{\partial q'}{\partial x}} = \frac{\bar{u}}{2} \frac{\partial \overline{q'^2}}{\partial x} = 0$$

yields with the aid of (10.26)

$$\frac{\partial A}{\partial t} + \nabla \cdot \mathbf{F} = D \tag{12.25}$$

where *wave activity*, A, and *dissipation*, D, are defined, respectively, as

$$A \equiv \frac{\rho_0 \overline{(q')^2}}{2 \partial \bar{q} / \partial y}, \quad \text{and} \quad \mathrm{D} \equiv -\frac{\rho_0 \overline{\mathrm{S'q'}}}{\partial \bar{\mathrm{q}} / \partial \mathrm{y}} \tag{12.26}$$

For linear planetary waves satisfying the quasi-geostrophic equations, it can be shown that

$$\mathbf{F} = \left(0, c_{gy}, c_{gz}\right) A \tag{12.27}$$

so that the EP flux is given by the wave activity times the group velocity in the meridional (y, z) plane. It is the flux of wave activity—not the flux of wave energy—that is fundamental for wave–mean-flow interaction.

Equation (12.25) shows that if dissipation and transience vanish, the EP flux divergence must vanish. Substitution into (12.1) then gives the *nonacceleration theorem*, which states that there is no wave-driven mean-flow acceleration for steady $(\partial A / \partial t = 0)$ and conservative $(D = 0)$ waves. The EP flux divergence, which must be nonzero for wave-induced forcing, is dependent on wave transience and dissipation.

In sudden stratospheric warmings the planetary wave amplitudes increase rapidly in time. During the Northern Hemisphere winter, quasi-stationary planetary waves of zonal wave numbers 1 and 2 are produced in the troposphere by orographic forcing. These waves propagate vertically into the stratosphere, implying a local increase in the wave activity. Thus, $\partial A / \partial t > 0$, implying from (12.25) that, for quasi-conservative flow, the flux of quasi-geostrophic potential

vorticity is negative and that the Eliassen–Palm flux field is convergent:

$$\rho_0 \overline{v'q'} = \nabla \cdot \mathbf{F} < 0 \tag{12.28}$$

Usually $D < 0$ also, so dissipation and wave growth both produce a convergent EP flux (i.e., an equatorward potential vorticity flux).

According to the transformed-Eulerian-mean zonal-momentum equation (12.1), EP flux convergence leads to a deceleration of the zonal-mean zonal wind, partially offset by the Coriolis torque $f\overline{v}^*$. As a result, the polar night jet weakens, allowing even more waves to propagate into the stratosphere. At some point, the mean zonal wind changes sign so that a critical layer is formed. Stationary linear waves can no longer propagate beyond the level where this occurs, and strong EP flux convergence and even faster easterly acceleration then occurs below the critical layer.

Figure 12.11a illustrates the deceleration of the zonal-mean wind due to the Eliassen–Palm flux convergence caused by upward propagation of transient planetary wave activity. Note that the deceleration is spread out over a broader range in height than the eddy forcing. This reflects the elliptical nature

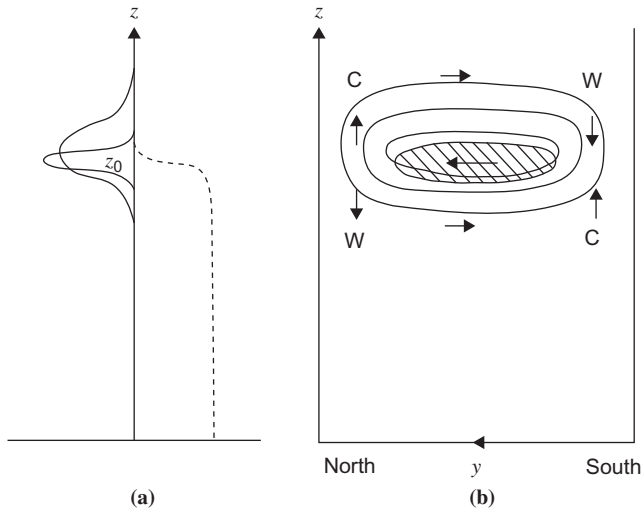

FIGURE 12.11 Schematic of transient wave, mean–flow interactions occurring during a stratospheric warming. (a) Height profiles of EP flux (*dashed line*), EP flux divergence (*heavy line*), and mean zonal flow acceleration (*thin line*); z_0 is the height reached by the leading edge of the wave packet at the time pictured. (b) Latitude–height cross-section showing region where the EP flux is convergent (*hatching*), contours of induced zonal acceleration (*lines*), and induced residual circulation (arrows). Regions of warming (W) and cooling (C) are also shown. (*From Andrews et al., 1987.*)

of the equation for mean zonal-wind acceleration that can be derived from the transformed Eulerian mean equations. Figure 12.11b shows the TEM residual meridional circulation and the pattern of temperature perturbation associated with the zonal wind deceleration. The thermal wind relation implies that a deceleration of the polar night jet leads to a warming in the polar stratosphere and a cooling in the equatorial stratosphere, with a compensating warming in the polar mesosphere and cooling in the equatorial mesosphere. Eventually, as more of the flow becomes easterly, waves can no longer propagate vertically. The wave-induced residual circulation then decreases, and radiative cooling processes are able to slowly reestablish the normal cold polar temperatures. Thermal wind balance then implies that the normal westerly polar vortex is also reestablished.

In some cases the wave amplification may be large enough to produce a polar warming but insufficient to lead to reversal of the mean zonal wind in the polar region. Such "minor warmings" occur every winter and are generally followed by a quick return to normal winter circulation. A "major warming" in which the mean zonal flow reverses at least as low as the 30-hPa level in the polar region seems to occur only about once every couple of years. If the major warming occurs sufficiently late in the winter, the westerly polar vortex may not be restored at all before the normal seasonal circulation reversal.

12.5 WAVES IN THE EQUATORIAL STRATOSPHERE

Section 11.4 discussed equatorially trapped waves in the context of shallow water theory. Under some conditions, however, equatorial waves (both gravity and Rossby types) may propagate vertically, and the shallow water model must be replaced by a continuously stratified atmosphere examine the vertical structure. It turns out that vertically propagating equatorial waves share a number of physical properties with ordinary gravity modes. Section 5.6 discussed vertically propagating gravity waves in the presence of rotation for a simple situation in which the Coriolis parameter was assumed to be constant and the waves were assumed to be sinusoidal in both x and y.

We found that such inertia–gravity waves can propagate vertically only when the wave frequency satisfies the inequality $f < \nu < N$. Thus, at the middle latitudes, waves with periods that are in the range of several days are generally vertically trapped—that is, they are not able to propagate significantly into the stratosphere. As the equator is approached, however, the decreasing Coriolis frequency should allow vertical propagation to occur for lower-frequency waves. Therefore, in the equatorial region there is a possibility for the existence of long-period, vertically propagating internal gravity waves.

As in Section 11.4, we consider linearized perturbations on an equatorial β plane. The linearized equations of motion, continuity equation, and first law of

thermodynamics can then be expressed in log-pressure coordinates as

$$\partial u'/\partial t - \beta y v' = -\partial \Phi'/\partial x \tag{12.29}$$

$$\partial v'/\partial t + \beta y u' = -\partial \Phi'/\partial y \tag{12.30}$$

$$\partial u'/\partial x + \partial v'/\partial y + \rho_0^{-1} \partial \left(\rho_0 w'\right)/\partial z = 0 \tag{12.31}$$

$$\partial^2 \Phi'/\partial t \partial z + w' N^2 = 0 \tag{12.32}$$

We again assume that the perturbations are zonally propagating waves, but we now assume that they also propagate vertically with vertical wave number m. Due to the basic state density stratification, there will also be an amplitude growth in height proportional to $\rho_0^{-1/2}$. Thus, the x, y, z, and t dependencies can be separated as

$$\begin{pmatrix} u' \\ v' \\ w' \\ \Phi' \end{pmatrix} = e^{z/2H} \begin{bmatrix} \hat{u}(y) \\ \hat{v}(y) \\ \hat{w}(y) \\ \hat{\Phi}(y) \end{bmatrix} \exp\left[i\left(kx + mz - \nu t\right)\right] \tag{12.33}$$

Substituting from (12.33) into (12.29) through (12.32) yields a set of ordinary differential equations for the meridional structure:

$$-i\nu\hat{u} - \beta y \hat{v} = -ik\hat{\Phi} \tag{12.34}$$

$$-i\nu\hat{v} + \beta y \hat{u} = -\partial \hat{\Phi}/\partial y \tag{12.35}$$

$$\left(ik\hat{u} + \partial \hat{v}/\partial y\right) + i\left(m + i/2H\right)\hat{w} = 0 \tag{12.36}$$

$$\nu\left(m - i/2H\right)\hat{\Phi} + \hat{w}N^2 = 0 \tag{12.37}$$

12.5.1 Vertically Propagating Kelvin Waves

For Kelvin waves the aforementioned perturbation equations can be simplified considerably. Setting $\hat{v} = 0$ and eliminating $\hat{w}$ between (12.36) and (12.37), we obtain

$$-i\nu\hat{u} = -ik\hat{\Phi} \tag{12.38}$$

$$\beta y \hat{u} = -\partial \hat{\Phi}/\partial y \tag{12.39}$$

$$-\nu\left(m^2 + 1/4H^2\right)\hat{\Phi} + \hat{u}kN^2 = 0 \tag{12.40}$$

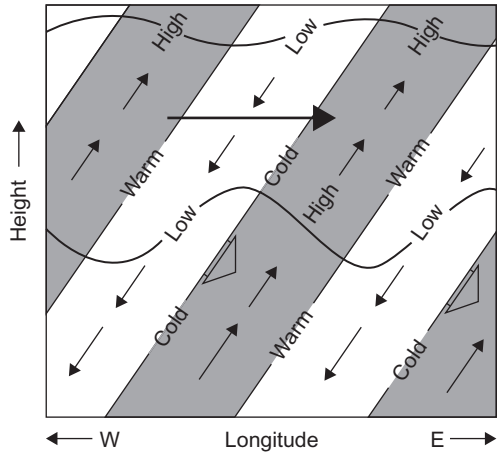

FIGURE 12.12 Longitude–height section along the equator showing pressure, temperature, and wind perturbations for a thermally damped Kelvin wave. *Heavy wavy lines* indicate material lines; *short black arrows* show phase propagation. Areas of high pressure are *shaded*. Length of the *small thin arrows* is proportional to the wave amplitude, which decreases with height due to damping. The *large shaded arrow* indicates the net mean flow acceleration due to the wave stress divergence.

Equation (12.38) can be used to eliminate Φ in (12.39) and (12.40). This yields two independent equations that the field of $\hat{u}$ must satisfy. The first of these determines the meridional distribution of $\hat{u}$ and is identical to (11.47). The second is simply the dispersion equation

$$c^2\left(m^2 + 1/4H^2\right) - N^2 = 0 \tag{12.41}$$

where, as in Section 11.4, $c^2 = (\nu^2/k^2)$.

If we assume that $m^2 \gg 1/4H^2$, as is true for most observed stratospheric Kelvin waves, (12.41) reduces to the dispersion relationship for internal gravity waves (5.66) in the hydrostatic limit ($|k| \ll |m|$). For waves in the stratosphere that are forced by disturbances in the troposphere, the energy propagation (i.e., the group velocity) must have an upward component. Therefore, according to the arguments of Section 5.4, the phase velocity must have a downward component. We showed in Section 11.4 that Kelvin waves must propagate eastward ($c > 0$) if they are to be trapped equatorially. However, eastward phase propagation requires $m < 0$ for downward phase propagation. Thus, the vertically propagating Kelvin wave has phase lines that tilt eastward with height as shown in Figure 12.12.

12.5.2 Vertically Propagating Rossby–Gravity Waves

For all other equatorial modes, (12.34) through (12.37) can be combined in a manner exactly analogous to that described for the shallow water equations

in Section 11.4.1. The resulting meridional structure equation is identical to (11.38) if we again assume that $m^2 \gg 1/4H^2$ and set

$$gh_e = N^2/m^2$$

For the $n = 0$ mode the dispersion relation (11.41) then implies that

$$|m| = N\nu^{-2}(\beta + \nu k) \tag{12.42}$$

When $\beta = 0$ we again recover the dispersion relationship for hydrostatic internal gravity waves. The role of the β effect in (12.42) is to break the symmetry between eastward ($\nu > 0$) and westward ($\nu < 0$) propagating waves. Eastward propagating modes have shorter vertical wavelengths than westward propagating modes. Vertically propagating $n = 0$ modes can exist only for $c = \nu/k > -\beta/k^2$. Because $k = s/a$, where s is the number of wavelengths around a latitude circle, this condition implies that for $\nu < 0$ solutions exist only for frequencies satisfying the inequality

$$|\nu| < 2\Omega/s \tag{12.43}$$

For frequencies that do not satisfy (12.43), the wave amplitude will not decay away from the equator and it is not possible to satisfy boundary conditions at the pole.

After some algebraic manipulation, the meridional structure of the horizontal velocity and geopotential perturbations for the $n = 0$ mode can be expressed as

$$\begin{pmatrix} \hat{u} \\ \hat{v} \\ \hat{\Phi} \end{pmatrix} = v_0 \begin{pmatrix} i\,|m|\,N^{-1}\nu y \\ 1 \\ i\nu y \end{pmatrix} \exp\left(-\frac{\beta\,|m|\,y^2}{2N}\right) \tag{12.44}$$

The westward-propagating $n = 0$ mode is generally referred to as the Rossby–gravity mode.[2] For upward energy propagation this mode must have downward phase propagation ($m < 0$) just like an ordinary westward-propagating internal gravity wave. The resulting wave structure in the x, z plane at a latitude north of the equator is shown in Figure 12.13. Of particular interest is the fact that poleward-moving air has positive temperature perturbations and vice versa so that the eddy heat flux contribution to the vertical EP flux is positive.

12.5.3 Observed Equatorial Waves

Both Kelvin and Rossby–gravity modes have been identified in observational data from the equatorial stratosphere. The observed stratospheric Kelvin waves are primarily of zonal wave number $s = 1$ and have periods in the range of 12 to

[2] Some authors use this term to describe both eastward and westward $n = 0$ waves.

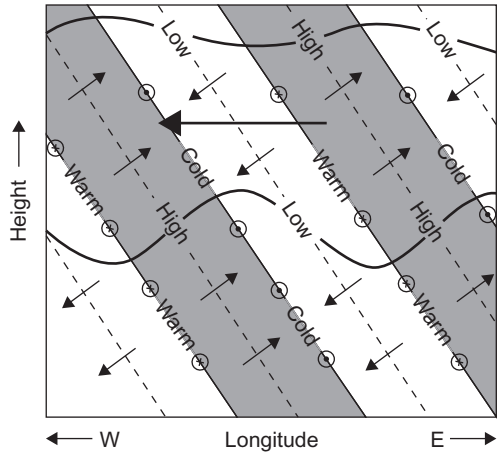

FIGURE 12.13 Longitude–height section along a latitude circle north of the equator showing pressure, temperature, and wind perturbations for a thermally damped Rossby–gravity wave. Areas of high pressure are *shaded*. *Small arrows* indicate zonal and vertical wind perturbations with length proportional to the wave amplitude. Meridional wind perturbations are shown by *arrows pointed into* the page (northward) and *out of the page* (southward). The *large shaded arrow* indicates the net mean flow acceleration due to the wave stress divergence.

20 days. An example of zonal wind oscillations caused by the passage of Kelvin waves at a station near the equator is shown in the form of a time–height section in Figure 12.14. During the observational period shown in Figure 12.14, the westerly phase of the quasi-biennial oscillation (see Section 12.6) is descending so that at each level there is a general increase in the mean zonal wind with increasing time. However, superposed on this secular trend is a large fluctuating component with a period between speed maxima of about 12 days and a vertical wavelength (computed from the tilt of the oscillations with height) of about 10 to 12 km.

Observations of the temperature field for the same period reveal that the temperature oscillation leads the zonal wind oscillation by 1/4 cycle (i.e., maximum temperature occurs prior to maximum westerlies), which is just the phase relationship required for upward-propagating Kelvin waves (see Figure 12.12). Additional observations from other stations indicate that these oscillations do propagate eastward at the theoretically predicted speed. Therefore, there can be little doubt that the observed oscillations are Kelvin waves.

The existence of the Rossby–gravity mode has been confirmed in observational data from the stratosphere in the equatorial Pacific. This mode is identified most easily in the meridional wind component, as v' is a maximum at the equator for the Rossby–gravity mode. The observed Rossby–gravity waves have $s = 4$, vertical wavelengths in the range of 6 to 12 km, and a period range of 4 to 5 days. Kelvin and Rossby–gravity waves each have significant amplitude only within about 20° latitude of the equator.

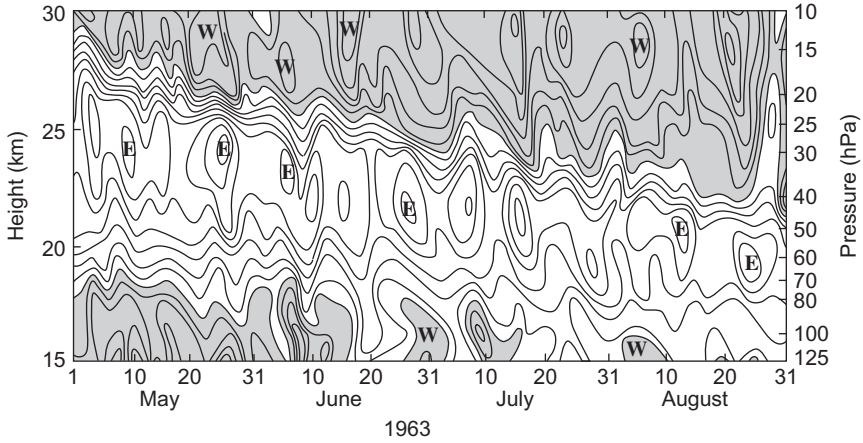

FIGURE 12.14 Time–height section of zonal wind at Canton Island (3°S). Isotachs at intervals of $5\,\mathrm{m\,s^{-1}}$. Westerlies are *shaded*. (*Courtesy of J. M. Wallace and V. E. Kousky.*)

A more complete comparison of observed and theoretical properties of the Kelvin and Rossby–gravity modes is presented in Table 12.1. In comparing theory and observation, it must be recalled that it is the frequency relative to the mean flow, not relative to the ground, that is dynamically relevant.

It appears that Kelvin and Rossby–gravity waves are excited by oscillations in the large-scale convective heating pattern in the equatorial troposphere. Although these waves do not contain much energy compared to typical tropospheric weather disturbances, they are the predominant disturbances of the equatorial stratosphere and, through their vertical energy and momentum transport, play a crucial role in the general circulation of the stratosphere. In addition to the stratospheric modes considered here, there are higher-speed Kelvin and Rossby–gravity modes, which are important in the upper stratosphere and mesosphere. There is also a broad spectrum of equatorial gravity waves, which appears to be important for the momentum balance of the equatorial middle atmosphere.

12.6 THE QUASI-BIENNIAL OSCILLATION

The search for periodic oscillations in the atmosphere has a long history. Aside, however, from the externally forced diurnal and annual components and their harmonics, no compelling evidence exists for truly periodic atmospheric oscillations. The phenomenon that perhaps comes closest to exhibiting periodic behavior not associated with a periodic forcing function is the quasi-biennial oscillation (QBO) in the mean zonal winds of the equatorial stratosphere. This oscillation has the following observed features.

TABLE 12.1 Characteristics of the Dominant Observed Planetary-Scale Waves in the Equatorial Lower Stratosphere

Theoretical description	Kelvin wave	Rossby–gravity wave
Discovered by	Wallace and Kousky (1968)	Yanai and Maruyama (1966)
Period (ground-based) $2\pi\omega^{-1}$	15 days	4–5 days
Zonal wave number $s = ka\cos\phi$	1–2	4
Vertical wavelength $2\pi m^{-1}$	6–10 km	4–8 km
Average phase speed relative to ground	+25 m s^{-1}	–23 m s^{-1}
Observed when mean zonal flow is	Easterly (maximum ≈ -25 m s^{-1})	Westerly (maximum $\approx +7$ m s^{-1})
Average phase speed relative to maximum zonal flow	+50 m s^{-1}	–30 m s^{-1}
Approximate observed amplitudes		
u'	8 m s^{-1}	2–3 m s^{-1}
v'	0	2–3 m s^{-1}
T'	2–3 K	1 K
Approximate inferred amplitudes		
Φ'/g	30 m	4 m
w'	1.5×10^{-3} m s^{-1}	1.5×10^{-3} m s^{-1}
Approximate meridional scales $(2N/\beta\lvert m\rvert)^{1/2}$	1300–1700 km	1000–1500 km

From Andrews et al., 1987.

1. Zonally symmetric easterly and westerly wind regimes alternate regularly with periods varying from about 24 to 30 months.
2. Successive regimes first appear above 30 km but propagate downward at a rate of 1 km mo^{-1}.
3. Downward propagation occurs without loss of amplitude between 30 and 23 km, but there is rapid attenuation below 23 km.
4. Oscillation is symmetric about the equator with a maximum amplitude of about 20 m s^{-1} and an approximately Gaussian distribution in latitude with a half-width of about 12°.

This oscillation is best depicted by means of a time–height section of the zonal wind speed at the equator as shown in Figure 12.15. It is apparent from this figure that the vertical shear of the wind is quite strong at the level where one regime is replacing the other. Because the QBO is zonally symmetric and causes only very small mean meridional and vertical motions, the QBO mean zonal wind and temperature fields satisfy the thermal wind balance equation. For the equatorial β plane this has the form—compare with (10.13):

$$\beta y \partial \overline{u}/\partial z = -RH^{-1}\partial \overline{T}/\partial y$$

For equatorial symmetry $\partial \overline{T}/\partial y = 0$ at $y = 0$, and by L'Hopital's rule thermal wind balance at the equator has the form

$$\partial \overline{u}/\partial z = -R(H\beta)^{-1}\partial^2 \overline{T}/\partial y^2 \tag{12.45}$$

Equation (12.45) can be used to estimate the magnitude of the QBO temperature perturbation at the equator. The observed magnitude of vertical shear of the mean zonal wind at the equator is $\sim 5\,\mathrm{m\,s^{-1}\,km^{-1}}$, and the meridional scale is $\sim 1200\,\mathrm{km}$, from which (12.45) shows that the temperature perturbation has an amplitude $\sim 3\,\mathrm{K}$ at the equator. Because the second derivative of temperature has the opposite sign to that of the temperature at the equator, the westerly and easterly shear zones have warm and cold equatorial temperature anomalies, respectively.

The main factors that a theoretical model of the QBO must explain are the approximate biennial periodicity, the downward propagation without loss of amplitude, and the occurrence of zonally symmetric westerlies at the equator. Because a zonal ring of air in westerly motion at the equator has an angular momentum per unit mass greater than that of Earth, no plausible zonally symmetric advection process could account for the westerly phase of the oscillation. Therefore, there must be a vertical transfer of momentum by eddies to produce the westerly accelerations in the downward-propagating shear zone of the QBO.

Observational and theoretical studies have confirmed that vertically propagating equatorial Kelvin and Rossby–gravity waves provide a significant fraction of the zonal momentum sources necessary to drive the QBO. From Figure 12.12 it is clear that Kelvin waves with upward energy propagation transfer westerly momentum upward (i.e., u' and w' are positively correlated so that $u'w' > 0$). Thus, the Kelvin waves can provide a source of westerly momentum for the QBO.

Vertical momentum transfer by the Rossby–gravity mode requires special consideration. Examination of Figure 12.13 shows that $\overline{u'w'} > 0$ also for the Rossby–gravity mode. The total effect of this wave on the mean flow cannot be ascertained from the vertical momentum flux alone, but rather the complete vertical EP flux must be considered. This mode has a strong poleward heat flux ($\overline{v'T'} > 0$), which provides an upward-directed EP flux contribution. This dominates over the vertical momentum flux, and the net result is that the

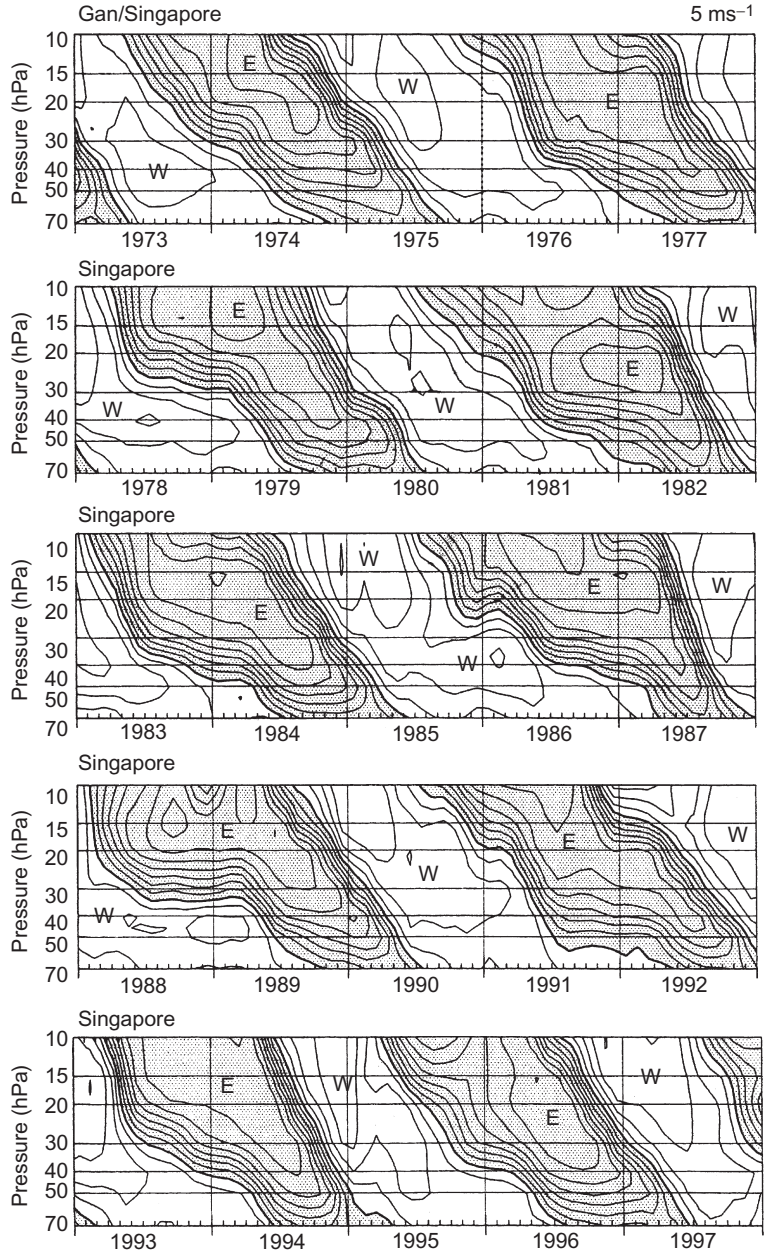

FIGURE 12.15 Time–height section of departure of monthly mean zonal winds (m s^{-1}) for each month from the long-term average for that month at equatorial stations. Note the alternating downward-propagating westerly (W) and easterly (E) regimes. (*After Dunkerton, 2003. Data provided by B. Naujokat.*)

Rossby–gravity mode transfers easterly momentum upward and can provide a momentum source for the easterly phase of the QBO. Observed Kelvin and Rossby–gravity wave momentum fluxes are not, however, sufficient to account for the observed zonal accelerations of the QBO. Additional wave sources, such as gravity waves generated by convective storms, must also contribute to the forcing of the QBO.

It was pointed out in Section 12.4 that quasi-geostrophic wave modes do not produce any net mean flow acceleration unless the waves are transient or are damped mechanically or thermally. Similar considerations apply to gravity waves and to the equatorial Kelvin and Rossby–gravity modes. Stratospheric waves are subject to thermal damping by infrared radiation, and to both thermal and mechanical damping by small-scale turbulent motions. Such damping is strongly dependent on the Doppler-shifted frequency of the waves.

As the Doppler-shifted frequency decreases, the vertical component of group velocity also decreases, and there is a longer time available for the wave energy to be damped as it propagates through a given vertical distance. Thus, eastward-propagating gravity waves and Kelvin waves tend to be damped preferentially in westerly shear zones, where their Doppler-shifted frequencies decrease with height. The momentum flux convergence associated with this damping provides a westerly acceleration of the mean flow, and thus causes the westerly shear zone to descend. Similarly, the westward-propagating gravity waves and Rossby–gravity waves are damped in easterly shear zones, thereby causing an easterly acceleration and descent of the easterly shear zone. We conclude that the QBO is indeed excited primarily by vertically propagating waves through wave transience and damping, which causes westerly accelerations in westerly shear zones and easterly accelerations in easterly shear zones.

This process of wave, mean-flow interaction can be elucidated by considering the heavy wavy lines shown earlier in Figures 12.12 and 12.13. These lines indicate the vertical displacement of horizontal surfaces of fluid parcels (material surfaces) by the velocity field associated with the waves. (For sufficiently weak thermal damping they are approximately the same as isentropic surfaces.) The wavy lines show that the maximum upward displacement occurs 1/4 cycle after the maximum upward perturbation velocity. In the Kelvin wave case (Figure 12.12), positive pressure perturbations coincide with negative material surface slopes. Thus, the fluid below a wavy material line exerts an eastward-directed pressure force on the fluid above. Because the wave amplitude decreases with height, this force is larger for the lower of the two material lines in Figure 12.12. There will thus be a net westerly acceleration of the block of fluid contained between the two wavy material lines shown in Figure 12.12.

For the Rossby–gravity wave, however, positive pressure perturbations coincide with positive slopes of the material lines. There is thus a westward-directed force exerted by the fluid below the lines on the fluid above as shown in Figure 12.13. In this case the result is a net easterly acceleration of the fluid contained between the two wavy material lines shown in Figure 12.13. Thus,

by considering the stresses acting across a material surface corrugated by the waves, it is possible to deduce the mean-flow acceleration caused by the waves without explicit reference to the EP fluxes of the waves.

How such a mechanism can cause a mean zonal flow oscillation when equal amounts of easterly and westerly momentum are transferred upward across the tropopause by the waves can be seen qualitatively by considering Figure 12.16. If initially, as shown in Figure 12.16a, the mean zonal wind is weak and westerly, the eastward-propagating waves will be preferentially damped at lower altitude and produce a westerly acceleration, which will move downward in time as the mean westerlies intensify and the wave-driven acceleration is concentrated at ever lower altitudes. The westward-propagating waves, however, initially penetrate to higher altitudes, where they produce easterlies, which also move downward in time. Eventually the westerlies are damped out as they approach the tropopause, and the stratosphere is dominated by easterlies so that the eastward-propagating waves can penetrate to high altitude and produce a new westerly phase. In this manner the mean zonal wind is forced to oscillate back and forth between westerlies and easterlies with a period that depends primarily on the vertical momentum transport and other properties of the waves, not on an oscillating external forcing.

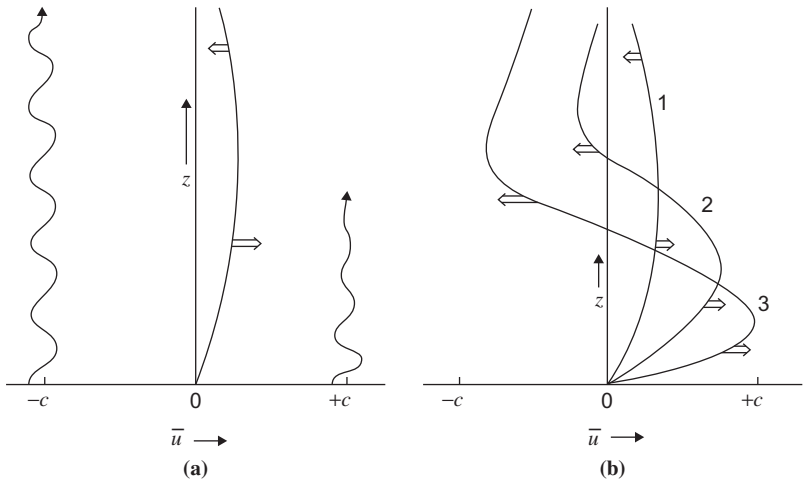

FIGURE 12.16 Schematic representation of wave-driven accelerations that lead to the zonal wind QBO. Eastward- and westward-propagating gravity waves of phase speeds $+c$ and $-c$, respectively, propagate upward and are dissipated at rates dependent on the Doppler-shifted frequency. (a) Initial weak westerly current selectively damps the eastward-propagating wave and leads to westerly acceleration at lower levels and easterly acceleration at higher levels. (b) Descending westerly shear zones block penetration of eastward-propagating waves, whereas westward-propagating waves produce descending easterlies aloft. *Broad arrows* show locations and direction of maxima in mean wind acceleration. *Wavy lines* indicate relative penetration of waves. (*After Plumb, 1982.*)

12.7 TRACE CONSTITUENT TRANSPORT

The study of global transport involves the motion of atmospheric tracers, which are defined as chemical or dynamical quantities that label fluid parcels. Chemical tracers consist of minor atmospheric species that have significant spatial variability in the atmosphere. Dynamical tracers (potential temperature and potential vorticity) are properties of the flow field that are conserved following the motion under certain conditions. These also can be useful for interpretation of transport.

12.7.1 Dynamical Tracers

Potential temperature, defined in (2.44), can be thought of as a label for the vertical position of an air parcel. Because the atmosphere is stably stratified, potential temperature increases monotonically with height (slowly in the troposphere and rapidly in the stratosphere as shown in Figure 12.17) and thus can be used as an independent vertical coordinate: the isentropic coordinates introduced in Section 4.6.1. A parcel moving adiabatically remains on a surface of constant potential temperature and can be "tagged" by its value of potential temperature. Thus the motion of such a parcel is two-dimensional when viewed in isentropic coordinates.

Potential temperature surfaces are quasi-horizontal, but they do move up and down in physical space with adiabatic changes in temperature. Thus, it is useful to reference trace constituent data to potential temperature, rather than pressure

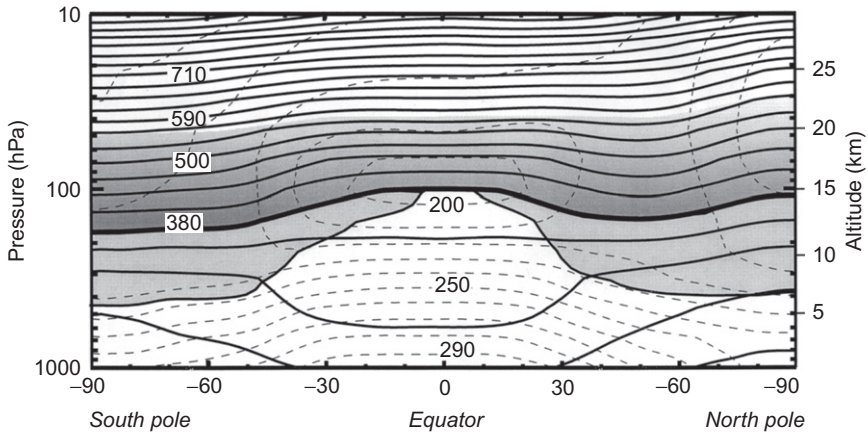

FIGURE 12.17 Latitude–height section showing January mean potential temperature surfaces (*solid contours*) and temperature (*dashed contours*). Heavy line shows the 380-K θ surface, above which all θ surfaces lie completely in the middle atmosphere. The *light shaded* region below the 380 K surface is the lowermost stratosphere, where Θ surfaces span the tropopause (shown by the *line* bounding the lower side of the shaded region). (*Courtesy of C. Appenzeller.*)

or altitude, as reversible variations at local altitudes or pressures caused by adiabatic vertical displacements associated with transient motions (e.g., gravity waves) are then accounted for.

The other commonly used dynamical tracer, potential vorticity (PV), is conserved for adiabatic, frictionless flow. As defined in equation (4.25), PV normally has a positive gradient in the meridional direction on an isentropic surface; it is negative in the Southern Hemisphere, zero at (or near) the equator, and positive in the Northern Hemisphere. PV has strong gradients in both height and latitude. Because a parcel moving in adiabatic frictionless flow conserves PV as well as potential temperature, its motion must lie parallel to isocontours of PV on isentropic surfaces. Rapid meridional transport implies production of strong PV anomalies as high polar values of PV are advected equatorward or low equatorial values are advected poleward. As discussed earlier, the meridional gradient of the background PV field resists meridional displacements through the production of Rossby waves. Thus, regions of strong PV gradients on isentropic surfaces can act as semipermeable "barriers" to transport. This PV barrier effect is one of the reasons that eddy diffusion is often not a good model for meridional transport.

Because PV depends only on the distribution of horizontal winds and temperatures on isentropic surfaces, its distribution can be determined from conventional meteorological observations. Thus, the evolution of PV on an isentropic surface can be used as a surrogate for the study of trace constituent transport on isentropic surfaces in circumstances in which there are inadequate observations of relevant chemical tracers. In addition, for dynamical studies, PV has the important property, not shared by other tracers, that it not only is advected by the flow, but actually determines the flow field. Thus, the distribution of PV on isentropic surfaces can be "inverted" to yield the wind and temperature fields. Changes in the PV distribution are then said to "induce" changes in the wind and temperature fields. In the quasi-geostrophic case the induced changes are required to maintain geostrophic and hydrostatic balance. More generally, such changes preserve a higher-order balance among the dynamical fields.

12.7.2 Chemical Tracers

Much can be learned about the nature of large-scale transport by considering the climatological distribution of quasi-conservative chemical tracers in the atmosphere. The distribution of such trace substances is dependent on the competition between dynamical and chemical processes. This competition can be approximately measured by comparing the characteristic dynamical and chemical timescales. *Chemical timescale* is the average time for replacement or removal of a tracer due to chemical sources and sinks. *Dynamical timescale* is the average time for advective and diffusive processes to transport the tracer from equator to pole or across a scale height in the vertical. The role of transport

in determining tracer climatology depends on the nature and distribution of tracer sources and sinks, and on the relative magnitudes of the timescales for dynamical and chemical processes.

If the chemical timescale is much shorter than the dynamical timescale, the tracer will be in photochemical equilibrium and transport does not directly influence its distribution. Transport can, however, play an important indirect role by partly determining the concentrations of other species that participate in the photochemical production or loss of the tracer in question.

If the chemical timescale is much longer than the dynamical timescale, the tracer will be passively advected by the flow field. In the absence of localized sources and sinks, such a tracer would eventually become well mixed due to the dispersive effects of transport. It is for this reason that species such as nitrous oxide (N_2O) tend to have uniform concentrations in the troposphere and are thus not useful for tropospheric transport studies.

When the chemical and dynamical timescales are comparable, the observed species concentration depends on the net effects of chemical sources and sinks and of transport. In many cases of interest, the ratio of chemical and dynamical timescales changes drastically between the troposphere and the stratosphere, and with altitude in the stratosphere. Tracers that have long lifetimes in the troposphere and the lower stratosphere are referred to as *long-lived tracers*, as the bulk of the tracer mass is contained in the troposphere and lower stratosphere, and the lifetime is determined mainly by the (slow) flux of the tracer to altitudes where the chemical timescales become comparable to or shorter than dynamical timescales.

12.7.3 Transport in the Stratosphere

Transport processes are conveniently divided between those that involve mean motions of the atmosphere, or *advection,* and those that may be characterized as turbulent, or diffusive in nature. In the case of point sources, such as volcanic eruptions, the distinction is quite clear; advection moves the center of mass of the plume along the direction of the average wind, whereas turbulent diffusion disperses the plume in the plane orthogonal to the average wind. On a global scale, however, the distinction between advective and diffusive processes is not always clear. Because the atmosphere is characterized by spatially and temporally varying motions with a wide range of scales, there is no obvious physical separation between “mean” and “turbulent” motions.

In practice, those transport processes that are explicitly resolved by the particular observational network or transport model being utilized are often regarded as the advective motions, whereas the remaining unresolved motions are assumed to be diffusive. The effects of the unresolved motions must then be parameterized in terms of the mean motions in some fashion. Usually this involves assuming that tracer fluxes by the unresolved motions are proportional to the gradient of the resolved tracer distribution. However, this approach is not

always physically justified. A major problem in the modeling of global transport is accurate representation of the contribution of the unresolved eddy motions to the total transport.

As discussed in Section 12.2, the global-scale residual meridional circulation in the middle atmosphere is driven by wave-induced zonal forces associated with Rossby waves and gravity waves. Not surprisingly, the residual circulation plays an essential role in the meridional and vertical transport of trace chemical constituents in the middle atmosphere. Additionally, the waves responsible for the zonal force that drives the residual circulation are also responsible for the quasi-isentropic stirring and mixing that is associated with wavebreaking. Thus, understanding of transport involves both eddy and mean-flow transport effects.

In dynamical studies it is usual to characterize a chemical constituent by the volume mixing ratio (or mole fraction), defined as $\chi \equiv n_T/n_A$, where n_T and n_A designate the number densities (molecules m^{-3}) for the trace constituent and air, respectively. The mixing ratio is conserved following the motion in the absence of sources and sinks and thus satisfies the simple tracer continuity equation

$$\frac{D\chi}{Dt} = S \tag{12.46}$$

where S designates the sum of all chemical sources and sinks.

As in the case of the dynamical variables discussed in Section 12.2, it is useful to define a longitudinally averaged mixing ratio $\overline{\chi}$ and a disturbance or eddy ratio χ' such that $\chi = \overline{\chi} + \chi'$. Again, it proves useful to use the residual mean meridional circulation $\left(\overline{v}^*, \overline{w}^*\right)$ defined in (10.16a,b). The zonal mean tracer continuity equation in the TEM framework can then be written as

$$\frac{\partial \overline{\chi}}{\partial t} + \overline{v}^* \frac{\partial \overline{\chi}}{\partial y} + \overline{w}^* \frac{\partial \overline{\chi}}{\partial z} = \overline{S} + \frac{1}{\rho_0} \nabla \cdot \mathbf{M} \tag{12.47}$$

Here, $\mathbf{M}$ represents the diffusive effects of the eddies, plus advective effects not represented by the residual meridional circulation. In models the term involving $\mathbf{M}$ is often represented by meridional and vertical eddy diffusion, with empirically determined diffusion coefficients.

To appreciate the role of the wave-induced global circulation in determining the distribution of long-lived tracers in the middle atmosphere, it is useful to consider a hypothetical atmosphere in which there are no wave motions and thus no wave-induced zonal force. In that case, as argued in Section 12.2, the middle atmosphere would relax to radiative equilibrium, the residual circulation would vanish, and the distribution of the tracer would be determined at each altitude by a balance between slow upward diffusion and photochemical destruction. Thus, tracer mixing ratio surfaces would, in an annual mean, tend to be close to horizontal. This is to be contrasted to observed distributions, which are characterized by mixing ratio surfaces that bow upward in the tropics and slope downward toward both poles (e.g., Figure 12.9).

As discussed in Section 12.2, the wave-induced global-scale circulation consists of upward and poleward motion across the isentropes in low latitudes, accompanied by diabatic heating, and downward motion across the isentropes at high latitudes, accompanied by diabatic cooling. Actual parcel trajectories, of course, do not follow the zonally averaged motion, but are influenced by the three-dimensional wave motion. Nevertheless the diabatic circulation defined by the mean diabatic heating and cooling closely approximates the global transport circulation. For seasonal and longer timescales the TEM residual circulation generally provides a good approximation to the diabatic circulation and is generally simpler to compute from standard meteorological analyses. For shorter-period phenomena in which the temperature tendency is large, the residual circulation is no longer a good approximation to the diabatic circulation.

The previous conceptual model of global transport is clearly supported by long-lived tracer observations as shown earlier in Figure 12.9. In middle latitudes there are regions in which tracer mixing ratio isopleths are nearly horizontal, reflecting the horizontal homogenizing role of meridional dispersion by planetary wavebreaking in the surf zone. The same processes also tend to homogenize the PV distribution on isentropes in the so-called surf zone in midlatitudes where Rossby wavebreaking tends to occur. The surf zone is bounded at both low and high latitudes by regions of strong meridional gradients of long-lived tracers and of PV. The existence of such gradients is evidence that there is only weak mixing into and out of the tropics and into and out of the polar winter vortex. Thus, these locations are sometimes referred to as "transport barriers." The strong PV gradients, strong winds, and strong wind shears that occur along the transport barriers at the subtropical and polar edges of the surf zone all act to suppress wavebreaking, and thus to minimize mixing and sustain the strong gradients at those locations.

SUGGESTED REFERENCES

Andrews, Holton, and Leovy, *Middle Atmosphere Dynamics* present a graduate-level treatment of the dynamics of the stratosphere and mesosphere.

Brasseur and Solomon's *Aeronomy of the Middle Atmosphere* has an excellent discussion of the chemistry of the stratosphere at an advanced level.

PROBLEMS

12.1. Suppose that temperature increases linearly with height in the layer between 20 and 50 km at a rate of 2 $K\,km^{-1}$. If the temperature is 200 K at 20 km, find the value of the scale height H for which the log-pressure height z coincides with actual height at 50 km. (Assume that z coincides with the actual height at 20 km and let $g = 9.81\ m\ s^{-2}$ be a constant.)

12.2. Find the Rossby critical velocities for zonal wave numbers 1, 2, and 3 (i.e., for 1, 2, and 3 wavelengths around a latitude circle). Let the motion be

referred to a β plane centered at 45°N, scale height $H = 7$ km, buoyancy frequency $N = 2 \times 10^{-2}$ s^{-1}, and infinite meridional scale ($l = 0$).

12.3. Suppose that a stationary linear Rossby wave is forced by flow over sinusoidal topography with height $h(x) = h_0 \cos(kx)$, where h_0 is a constant and k is the zonal wave number. Show that the lower boundary condition on the streamfunction ψ can be expressed in this case as

$$(\partial\psi/\partial z) = -hN^2/f_0$$

Using this boundary condition and an appropriate upper boundary condition, solve for $\psi(x, z)$ in the case $|m| \gg (1/2H)$ using the equations of Section 12.3.1. How does the position of the trough relative to the mountain ridge depend on the sign of m^2 for the limit $|m| \gg (1/2H)$.

12.4. Consider a very simple model of a steady-state mean meridional circulation for zonally symmetric flow in a midlatitude channel bounded by walls at $y = 0$, π/l and $z = 0$, π/m. We assume that the zonal mean zonal flow $\bar{u}$ is in thermal wind balance and that the eddy momentum and heat fluxes vanish. For simplicity, we let $\rho_0 = 1$ (Boussinesq approximation) and let the zonal force due to small-scale motions be represented by a linear drag: $\overline{X} = -\gamma\bar{u}$. We assume that the diabatic heating has the form $J/c_p = (H/R)J_0 \cos ly \sin mz$, and we let N and f be constants. Equations (12.1) through (12.4) then yield the following:

$$-f_0\bar{v}^* = -\gamma\bar{u}$$

$$+N^2HR^{-1}\bar{w}^* = +\bar{J}/c_p$$

$$\bar{v}^* = -\frac{\partial\overline{\chi}^*}{\partial z}; \quad \bar{w}^* = \frac{\partial\overline{\chi}^*}{\partial y}$$

$$f_0\partial\bar{u}/\partial z + RH^{-1}\partial\overline{T}/\partial y = 0$$

Assuming that there is no flow through the walls, solve for the residual circulation defined by $\overline{\chi}^*$, $\bar{v}^*$, and $\bar{w}^*$.

12.5. For the situation of Problem 12.4, solve for the steady-state zonal wind and temperature fields $\bar{u}$ and $\overline{T}$.

12.6. Find the geopotential and vertical velocity fluctuations for a Kelvin wave of zonal wave number 1, phase speed 40 m s^{-1}, and zonal velocity perturbation amplitude 5 m s^{-1}. Let $N^2 = 4 \times 10^{-4}$ s^{-2}.

12.7. For the situation of Problem 12.6 compute the vertical momentum flux $M \equiv \rho_0\overline{u'w'}$. Show that M is constant with height.

12.8. Determine the form for the vertical velocity perturbation for the Rossby–gravity wave corresponding to the u', v', and Φ' perturbations given in (12.44).

12.9. For a Rossby–gravity wave of zonal wave number 4 and phase speed -20 m s^{-1}, determine the latitude at which the vertical momentum flux $M \equiv \rho_0\overline{u'w'}$ is a maximum.

12.10. Suppose that the mean zonal wind shear in the descending westerlies of the equatorial QBO can be represented analytically on the equatorial β plane in the form $\partial u/\partial z = \Lambda \exp\left(-y^2/L^2\right)$ where $L = 1200$ km.

Determine the approximate meridional dependence of the corresponding temperature anomaly for $|y| \ll L$.

12.11. Estimate the TEM residual vertical velocity in the westerly shear zone of the equatorial QBO assuming that radiative cooling can be approximated by Newtonian cooling with a 20-day relaxation time, that the vertical shear is 20 m s^{-1} per 5 km, and that the meridional half-width is 12° latitude.

MATLAB Exercises

M12.1. The MATLAB script **topo_Rossby_wave.m** plots solutions for various fields for a stationary linear Rossby wave forced by flow over an isolated ridge. A β–plane channel model is used following the discussion in Section 12.3.1. Run the script for mean wind values of 5, 10, 15, 20, and 25 m s^{-1}. Describe how the geopotential and potential temperature perturbations change with changing mean wind speed. Explain these results based on the arguments given in Section 12.3.1.

M12.2. For the situation of Problem 12.4 let $J_0 = 10^{-6}$ s^{-3}, $N = 10^{-2}$ s^{-1}, $f = 10^{-4}$ s^{-1}, $l = 10^{-6}$ m^{-1}, $m = \pi/H$, where $H = 10^4$ m, and γ 10^{-5} s^{-1}. Make contour plots of the fields $\overline{u}, \overline{v}^*, \overline{w}^*, \overline{T}$ and discuss the relationship of these fields to the imposed diabatic heating.

M12.3. The MATLAB script **sudden_warming_model.m** provides an analog to the sudden stratospheric warmings on an extratropical β plane centered at 60°N. The amplitude of a single planetary wave of zonal wave number $s = 1$ or $s = 2$ is specified at the bottom boundary (taken to be the 16-km level), and a time integration is carried out to determine the evolution of the zonal mean wind in the stratosphere forced by the EP flux of the specified wave. For the cases $s = 1$ and 2, run the model for geopotential heights between 100 and 400 m at a 50-m interval. For each case note whether the flow tends toward steady state or repeated sudden warmings. Modify the code to plot the time–height evolution of the EP flux divergence for the case $s = 2$ and forcing of 200 m.

M12.4. The MATLAB script **qbo_model.m** is a simplified one-dimensional model of the equatorial QBO originally introduced by Plumb (1977). In this model the mean zonal flow is forced by two waves of equal amplitude at the lower boundary and equal and opposite phase speeds. The initial mean wind profile has a weak westerly shear. If the model is run for sufficiently weak forcing, the mean wind approaches a steady state, but for forcing greater than a critical amplitude, a downward-propagating oscillatory solution occurs, with period dependent on the amplitude of forcing. Run the script for a range of forcing between 0.04 and 0.40 and determine the approximate minimum forcing for a large-amplitude oscillatory motion to occur, and the dependence of period on the forcing amplitude. Modify the script to compute the time mean of the zonal wind over the course of several oscillations. Try a case in which the eastward forcing is 0.15 and the westward forcing is 0.075. How does the time mean wind change in this case?